# RESULTS

The activation of neurons is accompanied by alterations in the genomic (expression of immediate early genes; IEGs) and proteomic (posttranslational modification of proteins) level, respectively. Consequently, the visualisation of these processes may be used to map cells, which are activated during the process of social recognition. In spite of being commonly used to demonstrate activated neurons, IEG expression is not simply a generalised response to motor activity, novelty, or stress. It may be related to selected brain structures, and the factors that govern individual IEGs may vary between the brain areas (Guzowski et al., 2001). Consequently, the mapping of activated cells or cell groups in different brain areas is preferentially achieved by the combined detection of several IEGs.

In the present report the phosphorylation of proteins in general (phosphorylation at serine, threonine, and tyrosine residues), selected phosphoproteins like phosphorylated CREB (cAMP response element binding protein) and phosphorylated DARPP-32 (dopamine and cAMP- regulated phosphoprotein-32 kDa; Kozicz and Arimura, 2002; Ouimet et al., 1984) and the expression of immediate early genes like Homer, Narp, c-Fos, Egr.1, and Arc have therefore been visualised.

## 1. Morphological analysis of protein phosphorylation is no promising tool to follow neuronal activation during social interaction

Phosphorylation of proteins is a common response in activated neurons. It may be detected by visualising phosphorylated amino acids in proteins or by specific antibodies against selected phosphoproteins.

### 1.1 Phosphorylated amino acids

The visualisation of phosphorylated serine, tyrosine, and threonine residues (Fig. 4) demonstrated phosphorylated proteins throughout the main (MOB) and accessory olfactory bulb (AOB) in the juvenile stimulated (JS) rats. Proteins with phosphorylated serine residues (Fig. 4 B) were prominently displayed in the neuropil of the external plexiform layer (EPL) throughout the MOB.

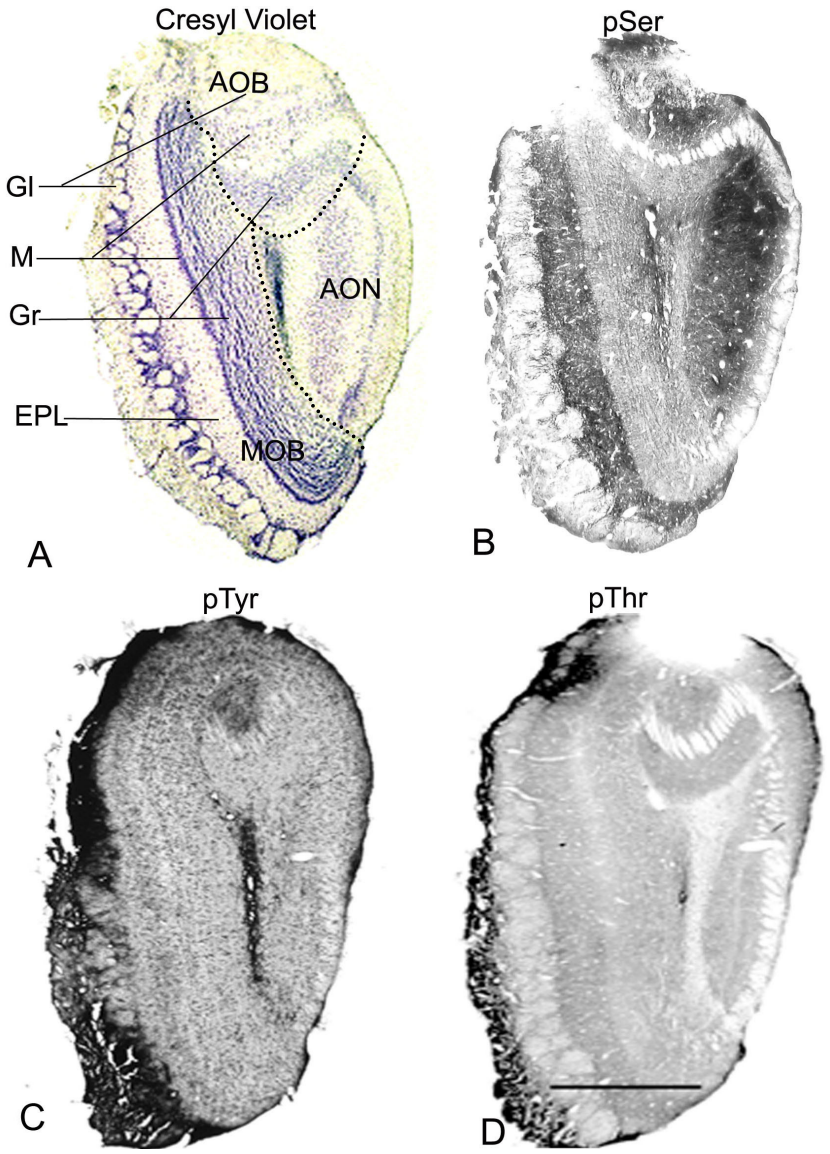


**Fig. 4. Patterns of phosphorylated proteins in the AOB of juvenile stimulated rats.**

The layered architecture of the main and the accessory olfactory bulb is readily visible in a cresyl violet stained coronal section (A). Dashed lines delineate the regions of the two olfactory bulbs. Phosphorylated proteins at serine residues are present through the neuropil (B). A strong immunoreactivity was found in the mitral (M) and external plexiform layer (EPL) of the main olfactory bulb while the granular (Gr) and the glomerular layers (Gl) show less intense immunoreactivity. Note the differences in the strength of serine-phosphorylated proteins in Gr and M/EPL. Tyrosine-phosphorylated proteins were displayed in many cells throughout the main and the accessory bulb (C). In the MOB, the highest densities of tyrosine-phosphorylated proteins were present in the glomerular layer while in the AOB, the mitral and glomerular cell layers showed more tyrosine-phosphorylated proteins. Threonine-phosphorylated proteins were mostly observed in the neuropil (C). In the MOB, the neuropil in Gl was weakly positive while the M and the EPL showed comparatively strong immunoreactivity.

**Fig.4. Patterns of phosphorylated proteins in the AOB of juvenile stimulated rats, continued.**

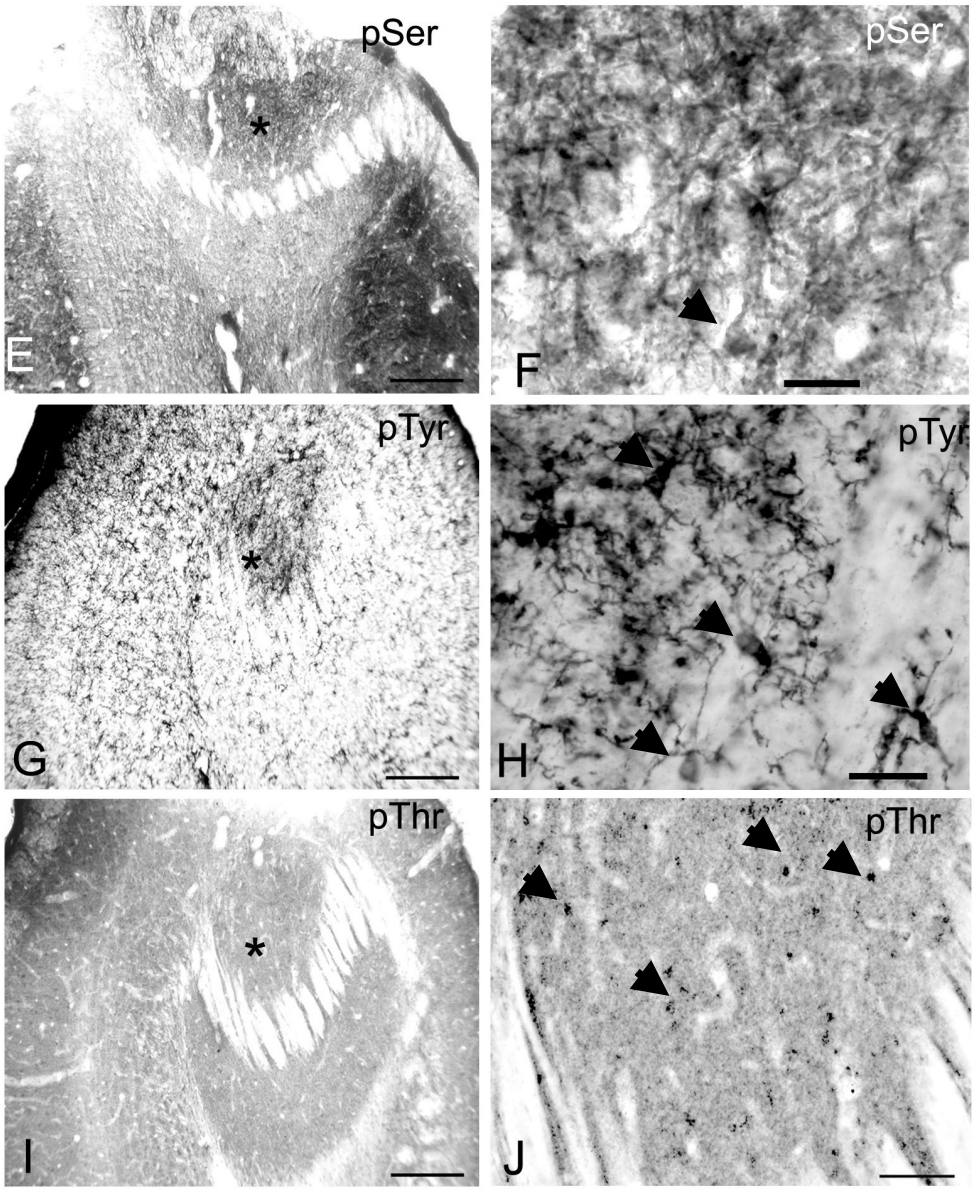


**Fig. 4 Patterns of phosphorylated proteins in the AOB of juvenile stimulated rats**

(Continued)
The neuropil in the granule cell layer was also weakly labelled with threonine-phosphorylated proteins. In the AOB, phosphorylated proteins with threonine residues were displayed in the neuropil. Figures E, G, and I are magnified images of areas indicated by rectangles in Fig. B, C, and D. Furthermore, Figures F, H, and J are photomicrographs of areas identified by asterisks in figures E, G, and I, respectively. At high magnification, serine phosphorylated proteins were observed mostly in the neuropil, and scarcely in neurons (arrowhead in F). Tyrosine-phosphorylated proteins were detected mostly in glial and neuronal cells (arrowheads in H). Threonine-phosphorylated proteins were found mainly in the neuropil throughout the main and accessory olfactory bulb, and in cells (arrowheads in J). Abbreviations: AOB: accessory olfactory bulb; AON: anterior

olfactory nucleus; EPL: external plexiform layer; Gl: glomerular layer; Gr: granule cell layer; M: mitral cell layer; MOB: main olfactory bulb. Scale bar 1000 µm D, 500 µm I, 20 µm F and J, 50 µm H.

The neuropil in the external plexiform layer was considerably stained with serine-phosphorylated proteins compared to the granule cell layer (Gr). Serine-phosphorylated proteins were mainly detected in the mitral cell (M) dendrites while immunopositivity in mitral cell soma was rarely distinguishable. Nevertheless, scattered immunoreactive cells with serine-phosphorylated proteins were detected in the mitral cell layer of the MOB (data not shown). Like in the MOB, in the AOB, the mitral cell dendrites extending towards the glomerular layer (Gl) and the neuropil were strongly stained with serine-phosphorylated proteins (Fig. 4 E and F). In the AOB, the granule cell layer was only weakly labelled with serine-phosphorylated proteins. A few, if any, cell soma were distinguishable in the mitral cell layer in the AOB (Fig. 4 F). The pattern of serine phosphoproteins in the control group was similar to the JS group (data not shown).

Studying tyrosine-phosphorylated proteins revealed much immunoreactivity in neuronal and glial cells throughout the main and accessory olfactory bulb of the JS group (Fig. 4C, G and H). In the MOB, the highest densities of tyrosine-phosphorylated proteins were observed in the glomerular layer while in the AOB, the M/EPL and glomerular layer were stained strongly with tyrosine-phosphorylated proteins (Fig. 4 C, G and H). The same pattern of phosphotyrosine proteins was observed in the control animals.

Threonine-phosphorylated proteins were frequently observed in the neuropil (Fig. 4 D, I and J) of JS rats. In contrast to the weakly stained glomerular layer, the external plexiform layer in the MOB was labelled mildly. Similar to serine phosphorylation, the granule cell layer showed a weak staining with threonine-phosphorylated proteins. In the AOB, the neuropil in the M/EPL and granular cell layers showed signals of phosphorylated proteins with threonine residues. In addition to the neuropil, some weakly labelled neural cells could be distinguished in the mitral and external plexiform layer (arrowheads in Fig. 4 J).

Visualising the phosphorylated proteins with serine, threonine, and tyrosine residues in the control animals revealed a pattern of immunoreactivity in the MOB and AOB similar to that of the JS group. The pattern of amino acid phosphorylation did not differ between the two groups of rats. Consequently, phosphorylated amino acids could not provide quantifiable

and reliable data necessary for mapping neuronal activities caused by individual recognition processes. Therefore, phosphorylated proteins such as CREB and DARPP-32 were studied next.

### 1.2 Visualisation of DARPP-32 and pCREB

Phosphorylated DARPP-immunoreactive neurons were observed only in the ependymal and subependymal layers of the olfactory bulb as well as in the anterior olfactory nucleus of both JS and control groups (Fig. 5 A-C). Phosphorylated DARPP-ir cells were not detected in the AOB of any group of rats.

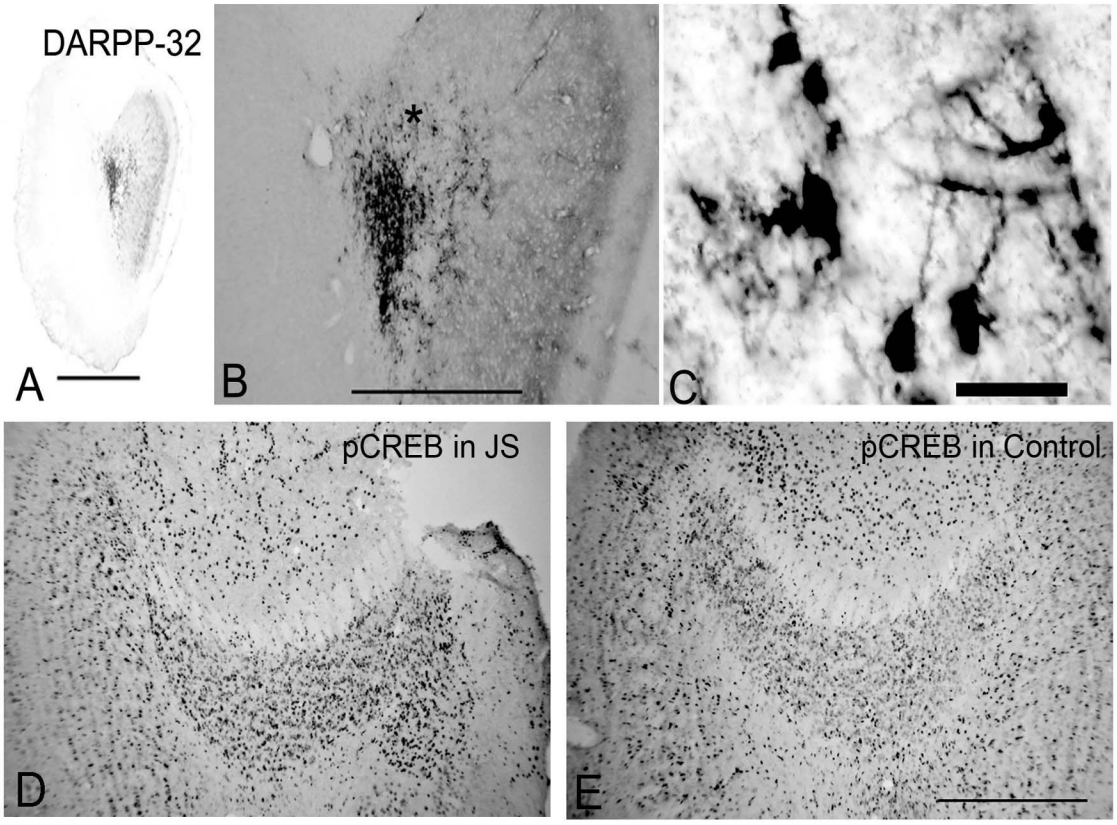


**Fig. 5 Patterns of phosphorylated DARPP-32 and CREB proteins in the olfactory bulb**

Immunopositive cells for phosphorylated DARPP-32 were observed in the ependymal and subependymal zone and in the anterior olfactory nucleus of the JS group (A-B). No immunoreactive cell was found in the main or accessory olfactory bulbs. A highly magnified photomicrograph (C) shows immunopositive neurons and axonal fibres in the ependymal zone of the olfactory bulb. Phosphorylated CREB-ir neurons are clearly discernible in the AOB of JS (D) and control (E) rats. Numerous strongly labelled pCREB-ir neurons were

observed in the granular cell layer, mitral cell layer and external plexiform layer. Bar represents 1000 µm in A, 200 µm in B, 50 µm in C, 500 µm in E.

In JS, as well as control animals, phosphorylated CREB (pCREB) positive cells were frequently observed in the MOB and AOB (Fig. 5 D and E). In the MOB of the JS group, the granular cell layer displayed numerous strongly labelled pCREB-ir neurons while the mitral cell layer showed rare weakly stained mitral cells (data not shown). In the AOB, granular cell layer showed a high density of pCREB immunoreactive neurons. The M/EPL and glomerular layers of the AOB displayed a dense population of pCREB-ir neurons. In the control animals, the pattern of pCREB-ir neurons was similar to that of the JS group. The presence of a dense population of phospho-CREB immunoreactive neurons in the MOB and the AOB of the two groups of animals suggests pCREB is unspecific to the social recognition paradigm. As there were no evident differences in protein phosphorylation between JS and control animals, the analysis of phosphorylated proteins cannot be used to monitor brain areas activated during the social recognition paradigm.

### 1.3 Investigation of immediate early genes expression

We then investigated the expression patterns of IEG-encoded proteins. The IEGs c-Fos, early growth response factor-1 (Egr.1), activity-regulated cytoskeleton associated protein (Arc), JUN-B, Fos-B, Narp (neuronal activity regulated pentraxin), and Homer 1a were selected for this purpose.

Using a polyclonal antibody against Homer proteins 1a, 1b, and 1c, only a few, weakly labelled Homer positive neurons were observed in the MOB and AOB of both the JS and control group of animals (data not shown). In the MOB, these neurons were located in the granular cell layer. Furthermore, rarely scattered positive neurons were detected in the external plexiform layer (data not shown). In the AOB of the JS group, a few immunoreactive neurons were identified in the granular cell layer and M/EPL. In the control animals, the expression of Homer was similar to that in the JS group. A few weakly stained immunopositive neurons were detected in the granular cell layer of the MOB and AOB, and rarely scattered positive cells were displayed in the M/EPL of both areas. Thus, there was no difference between the expression patterns of Homer between the two groups.

The analysis of the expression pattern of Narp (data not shown) revealed Narp-immunoreactive neurons in the mitral cell layer in the MOB of the JS group. There was no immunoreactivity in other layers of the MOB. The same pattern of Narp-immunoreactive neurons was observed in the mitral cell layer of the AOB of the JS group. Similarly, Narp-immunoreactive neurons were observed only in the mitral cell layer in the MOB and AOB of the control group. There was no difference between the patterns of Narp expression between the JS and the control group of animals.

Expression of Jun-B was displayed mainly in the granular cell layer, mitral cell layer and glomerular layer in the MOB of the JS group (data not shown). Some Jun-B immuno-positive neurons were identified in the EPL. In the AOB of the JS group, like in the MOB, the granule cell layer showed many immunostained neurons. Relatively few immunopositive neurons were observed in the M/EPL. In the MOB of the control group, the expression pattern of Jun-B was similar to that in the JS group. Numerous immunoreactive cells were displayed in the Gr, M, and Gl. Furthermore, a few immunostained neurons for Jun-B were observed in the EPL. In the AOB of the control rats, the Gr showed many immunoreactive neurons comparable to that found in the JS group while less Jun-B expressing neurons were detected in the M/EPL. Thus, there was no difference in the Jun-B expression between the JS and the control group of rats.

Immunolabelled neurons for Fos-B (data not shown) were observed frequently in the granule cell layer of the MOB in JS rats. Some immunoreactive neurons were also observed in the mitral cell layer, and a few weakly stained neurons were visualised in the Gl. In the AOB, the granule cell layer displayed many Fos-B immunoreactive neurons while the M/EPL showed a few immunostained cells. In the MOB of control rats, the expression pattern of Fos-B was similar to that of the JS group, showing many immunoreactive cells in Gr and less in the mitral cell layer. A few weakly labelled cells occurred in the glomerular layer. In the AOB, control rats displayed many Fos-B immunopositive cells in Gr and a few Fos-B expressing neurons in the M/EPL. The expression pattern of Fos-B, like that of Homer, Narp, and JUN-B, was not specific to the social stimulation processing. Therefore, these patterns cannot be used for mapping neuronal activity in the relevant brain structures.

## 2. Exposure of adult male rats to juvenile rats caused expression of c-Fos, Egr.1, and Arc in the accessory olfactory bulb

Among a variety of phosphoproteins and IEG products studied to map neuronal activities in the brain during the social recognition process, the expression patterns of three widely used IEG-encoded proteins, namely c-Fos, Egr.1, and Arc, were specifically altered when exposing rats to an unfamiliar juvenile.

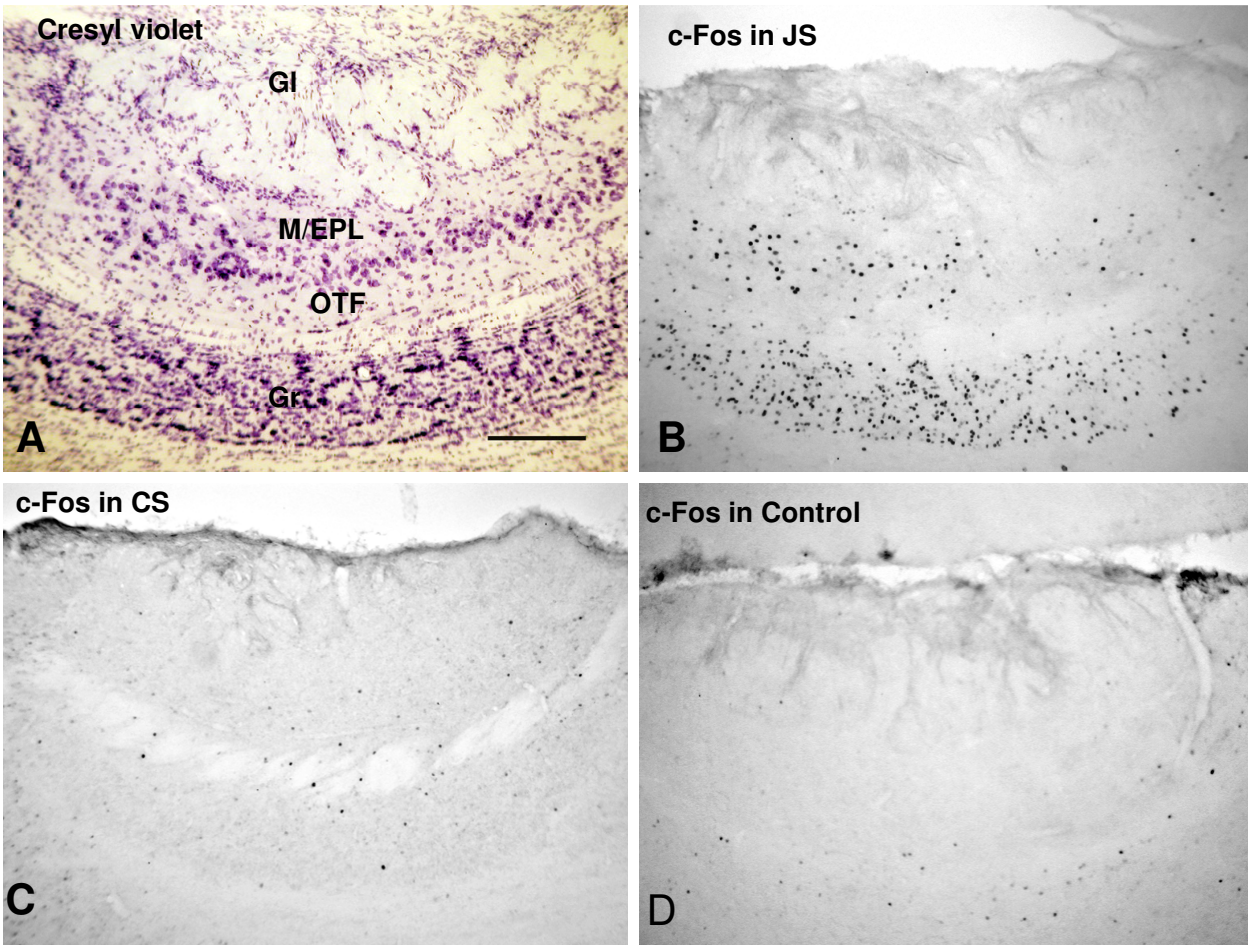


**Fig. 6 Fos expression in the accessory olfactory bulb of three groups of rats**

Juvenile stimulation caused high expression of the c-Fos protein in the AOB (JS). By contrast, neither the control group nor carvone stimulated rats showed a similar neural activation. A. Cresyl violet staining. The sagittal section shows the different layers of the AOB. B. Juvenile stimulation. Many c-Fos-ir cells are displayed in Gr and M/EPL. C. Carvone stimulation. Few cells are displayed in Gr and M/EPL layers. D. Control. Only occasionally, c-Fos-positive cells were observed in the granule cell layer. Abbreviation: M/EPL: mitral cell layer/ external plexiform layer; GL: glomerular layer; Gr: granule cell layer; OTF: olfactory tract fibres. Scale bar 200 µm.

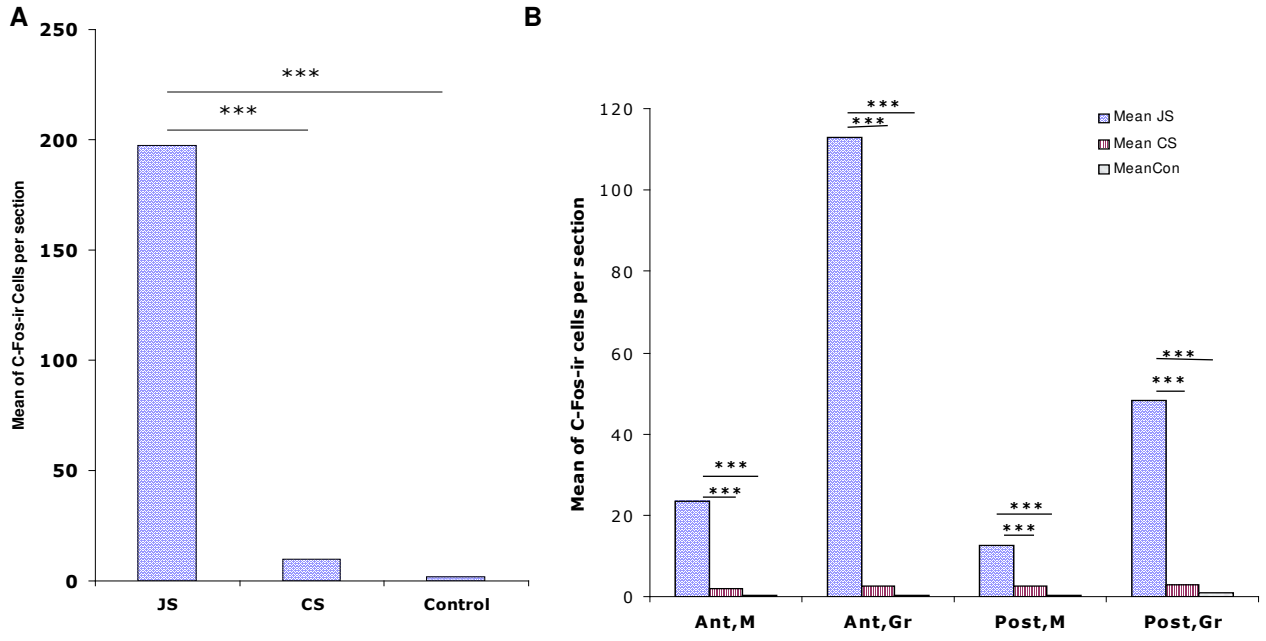


**Fig. 7 Fos expression in the AOB of three groups of rats**

Average numbers of c-Fos positive cells in the AOB of JS, CS and control group are shown in diagram (A). Juvenile stimulation caused significantly more c-Fos expression in the AOB, compared to the other two groups. The analysis of the anterior-posterior distribution pattern of the c-Fos expression in the JS group indicated that either in the granular or mitral cell layer, about two-thirds of the c-Fos-ir cells were located in the anterior part of the AOB (B). Either anterior or posterior parts of the mitral cell layer and the granular cell layer of the JS group expressed significantly more c-Fos than identical areas in the two other groups of rats did. Abbreviations: JS: juvenile stimulated group, CS: Carvone stimulated group, M: mitral cell layer, Gr: granule cell layer, Ant: anterior, Post: posterior, **: $P$=0.01, ***: $P$=0.001.

In the juvenile stimulated rats, intense c-Fos-ir cells were observed in the mitral and granule cell layer of the AOB (Fig.6 B) while the control group displayed only very few c-Fos immunoreactive cells in these areas (Fig. 6 C). To verify whether this neuronal activation was specifically caused by social (pheromonal) stimulation, c-Fos expression was investigated in another group of rats, the carvone stimulated (CS) group. This group of rats very rarely showed scattered c-Fos-ir neurons in the AOB (Fig. 6 D), which did not significantly differ from the control group. By contrast, c-Fos immunoreactive cells were frequently observed in the MOB of CS rats (data not shown).

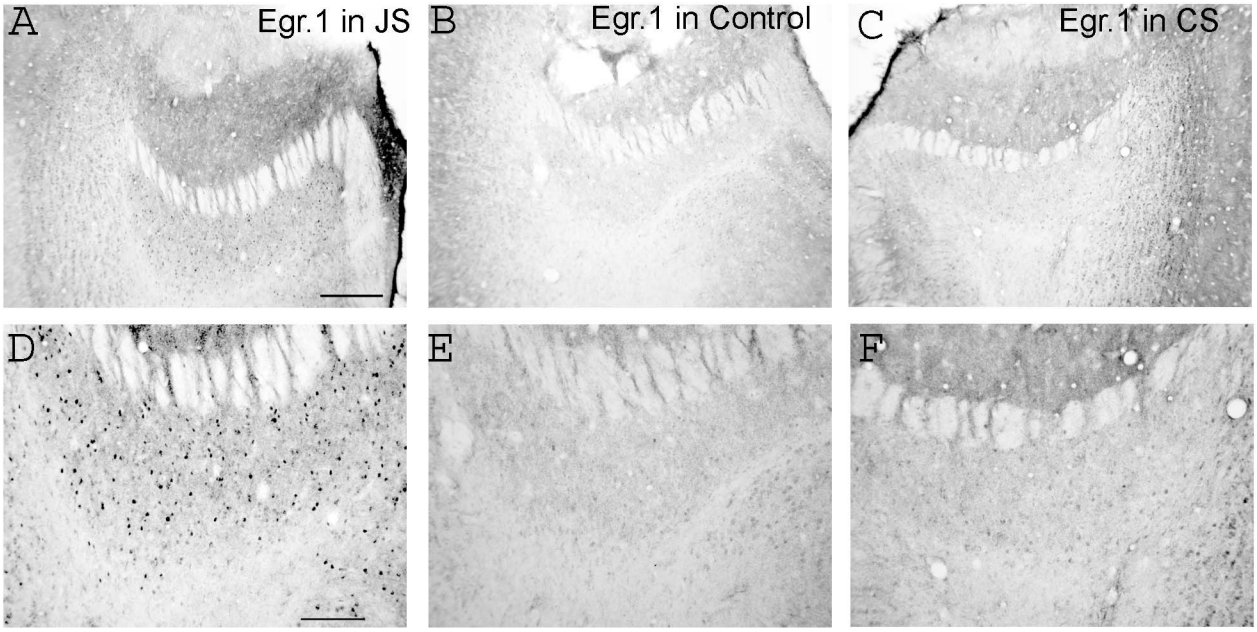


**Fig. 8 Expression of Egr.1 in the AOB of three groups of rats**

Juvenile stimulation caused a high expression of Egr.1 protein in the accessory olfactory bulb (A) while in the control group or in carvone-exposed animals no similar effect was observed (B and C). Higher magnification images of the granule cell layer in A-C are shown in D-F. Only few Egr.1-ir neurons were detected in the AOB of control rats (B and E). A few very weakly labelled neurons were observed in the AOB of carvone stimulated rats. Scale bar 200 µm in A, 100 µm in D.

The quantification of immunoreactive cells and subsequent statistical analysis (Fig. 7 A) showed significantly more c-Fos expression in the AOB of juvenile stimulated animals compared with control ($P<0.001$) and carvone stimulated groups ($P<0.001$).

The investigation of c-Fos expression revealed that the different cellular layers of the AOB were activated differently during juvenile stimulation. In the AOB of the JS group, the densest pattern of c-Fos-immunoreactivity was observed in the granule cell layer while only rarely weakly labelled c-Fos-ir neurons were observed in the glomerular layer. In the JS group, both mitral and granule cell layers displayed numerous c-Fos-ir cells. However, the mitral cell layer contained less than one-third of all immunoreactive cells in the AOB while granule cells contained approximately two-thirds of c-Fos-ir cells (Fig. 7 B). Still, a significantly increased number of c-Fos-ir cells were observed in JS compared to the two other groups, both in mitral ($P<0.001$) and granule ($P<0.001$) cell layers (Fig.7 D). In

contrast to the low level of Fos activation in the AOB of the CS group, neuronal activity was considerably higher in the MOB of this group than in that of the JS group (data not shown).

Juvenile stimulation furthermore resulted in an increased expression of Egr.1 selectively in the granule cell layer of the accessory olfactory bulb while the AOB of other groups of rats displayed only a few scattered Egr.1-ir neurons (Fig.8). A similar expression pattern was observed for Arc in the AOB of JS rats (Fig. 9). In contrast to the control and CS groups, in JS rats many Arc-ir neurons in the granule cell layer of the AOB were evident. While c-Fos-ir cells were observed in granule and mitral cell layers, the expression of Egr.1 and Arc was restricted to the granule cell layer (Fig.10). Furthermore, Arc-immunoreactivity was observed in the cell bodies and dendrites of granule cells.

**3. Juvenile stimulation resulted in different patterns of IEG induction in the anterior and posterior parts of the AOB.**

To study the different patterns of neuronal activation in the anterior and posterior parts of the AOB in the JS group, these two parts were distinguished by immunohistochemical labelling of adjacent sections with antibodies against the G protein: $\alpha$ subunits $G\alpha i2$ to identify the anterior part of the AOB, and $G\alpha o$ to detect the posterior part.

The photomicrographs in Fig. 11 show examples suggesting an uneven distribution of c-Fos immunolabelled cells in the anterior and posterior parts of the AOB after the rats had been exposed to a juvenile stimulus. Cells immunoreactive to c-Fos, Egr.1, and/or Arc seemed to be more abundant in the anterior part of the AOB than in the posterior part. To analyse different patterns of neuronal activation in the anterior and posterior parts of the AOB in the JS rats, c-Fos-ir cells in these two parts were quantified.

The c-Fos-ir cells in the anterior/posterior parts of the mitral and granule cell layers of each section were analysed. Statistical analysis showed a significantly higher expression of c-Fos in the anterior part of the AOB (Fig. 7 B) than in the posterior part. Furthermore, statistical analyses[I1] showed a significant increase ($t=2.87$, $df=34$, $P=0.007$) in the c-Fos-ir cells in the anterior part of the AOB. In the mitral cell layer, 60% of the quantified c-Fos-ir cells were observed in the anterior part of the AOB and the rest were observed in the posterior part. Similarly, in the granule cell layer, 65% of the c-Fos-ir cells were quantified

in the anterior AOB. On average, 64% of the immunoreactive cells were observed in the anterior part of the AOB. Differences in the number and density of c-Fos immunoreactivity between the anterior and posterior parts of the AOB were confirmed by a one-way ANOVA followed by Scheffe's multiple comparison test ($F$= 13.775, d.f. =3,100, $P$=0.000). In summary, the results indicate a significant increase in the IEG expression in the AOB of the JS rats, and a preferential neuronal activation in the anterior part of the AOB. Additionally, the expression of Arc and Egr.1 also showed a tendency to localise preferentially in the anterior part of the AOB. However, this observation was not verified by quantification analysis. Also, Egr.1 and Arc were restricted to the granule cell layer.

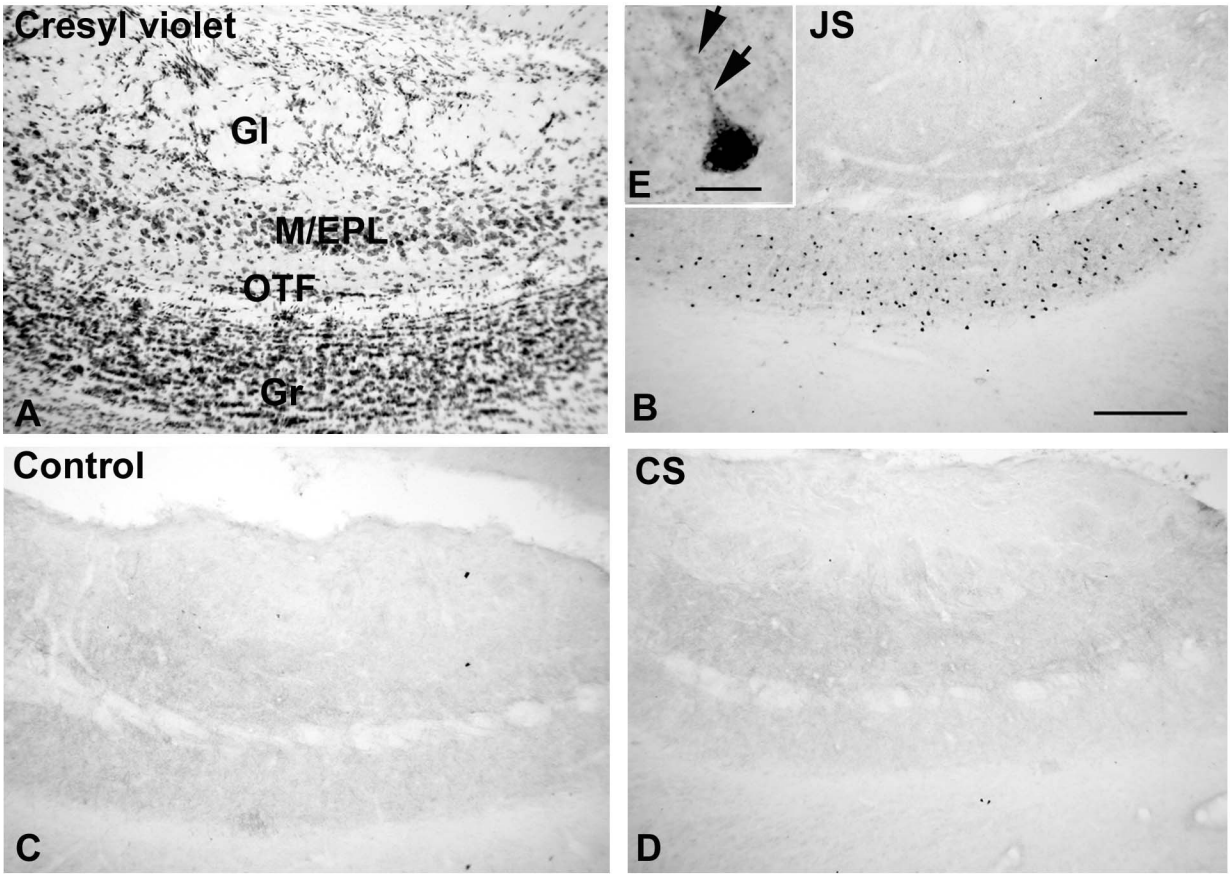


**Fig. 9 Arc expression in the accessory olfactory bulb of three groups of rats**

Juvenile stimulation induced Arc protein in the AOB (B) while in the control group (C) or carvone stimulated animals (D) there was no evidence of Arc expression in the AOB. Note that the Arc expression in the JS group was restricted to the granular cell layer and more predominant in the anterior part of the AOB. Arc-immunoreactivity was also observed in the dendrites of granule cells, arrowheads in E. A. Cresyl violet

staining of the AOB indicates its different cellular architecture. Abbreviations: M/EPL: mitral cell layer/ external plexiform layer, Gl: glomerular layer; Gr: granule cell layer. Scale bar 200 µm B, 10 µm in E .

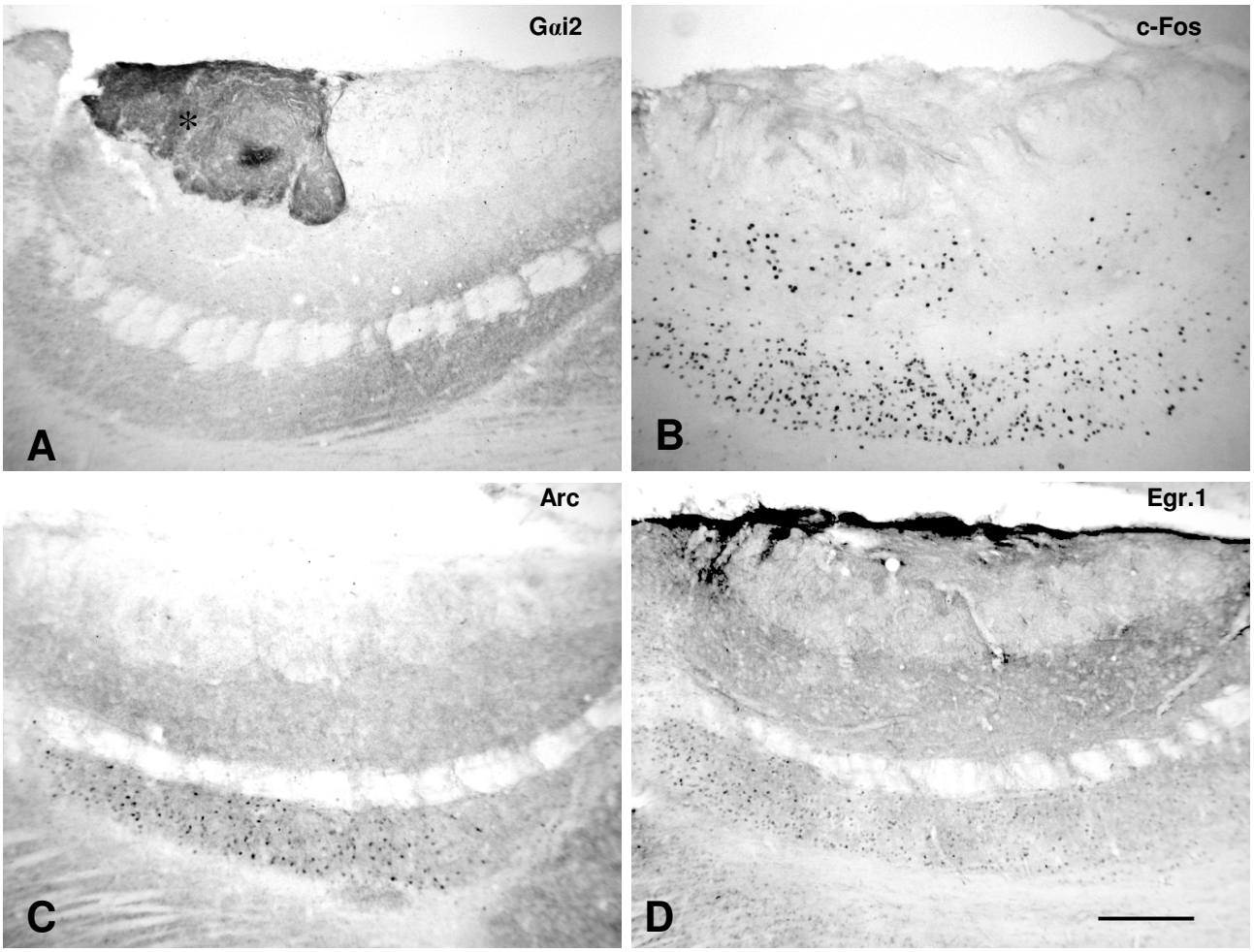


**Fig. 10 Anterior-posterior distribution patterns of c-Fos, Arc, and Egr.1 immunoreactivity in the AOB of JS rats**

The anterior part of the AOB is indicated by an asterisk in the Gαi2 immunostained sagittal section (A). Sections immunolabelled with antibodies against c-Fos, Arc, and Egr.1 are shown in B, C, and D respectively. Juvenile stimulation caused c-Fos expression in the AOB. Although immunopositive c-Fos cells were observed in both mitral cell layers, the majority of c-Fos-ir cells were observed in the anterior portion of the granule cell layer of the AOB. Arc and Egr.1 immunopositive cells were also concentrated in the anterior part of the AOB, but were restricted to the granule cell layer. Scale bar 200 µm.

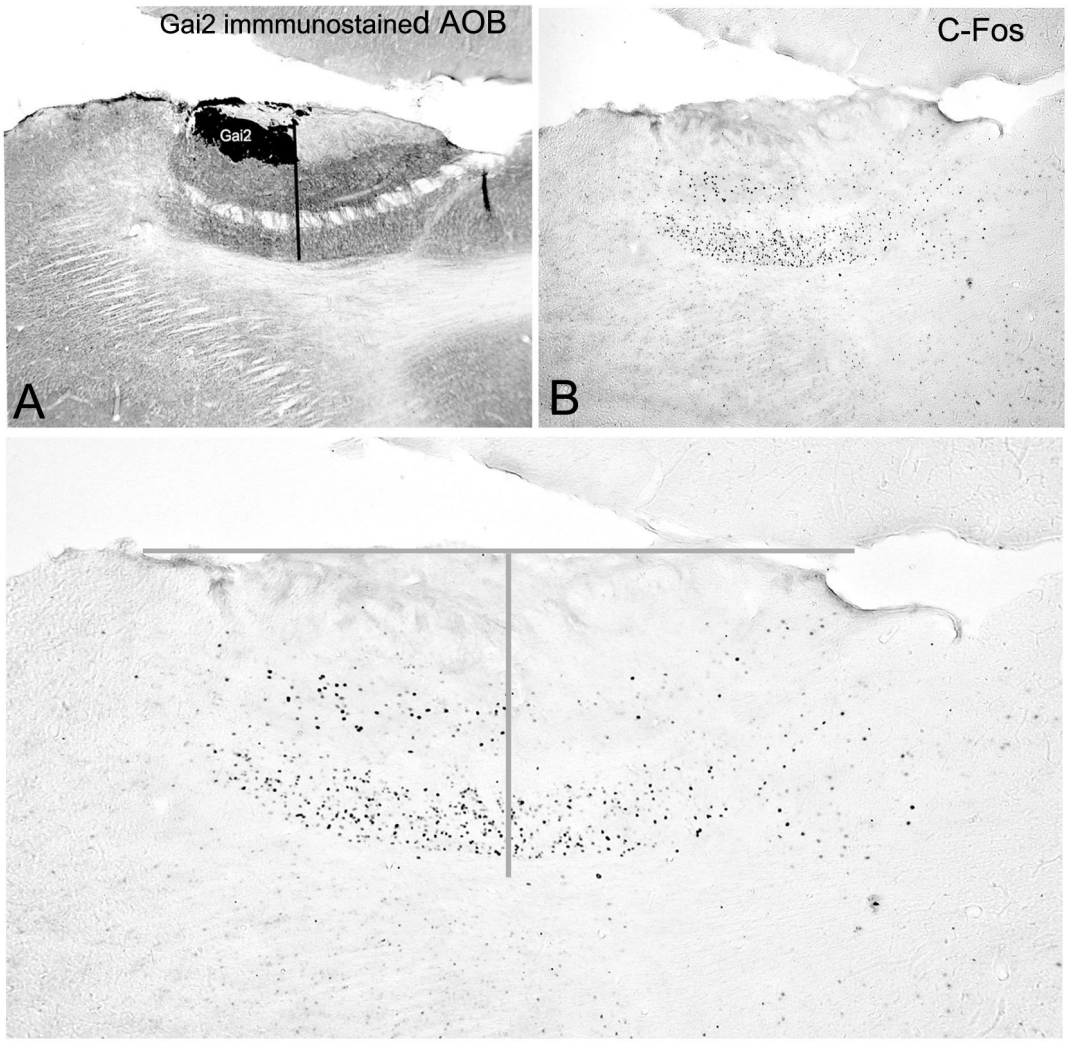


**Fig. 11 Quantification of c-Fos immunoreactive cells in the anterior and posterior parts of the AOB**

The anterior part of the AOB can easily be recognised in the immunostained sagittal section with antibody against Gαi2 (A). The adjacent section is immunolabelled with antibody against c-Fos (B). The anterior/posterior parts of the image of the Gαi2 stained section was detected. Then, by merging it with the image of the c-Fos labelled section, the anterior/posterior parts of the AOB were distinguished in the c-Fos section (C). Subsequently, the c-Fos-ir cells in the two parts were quantified and analysed.

## 4. Social stimulation caused high expression of IEGs in the amygdala

The expression patterns of IEGs in the amygdala were studied since the amygdala is one of the main projection targets of the AOB. More than 25 individual nuclei located in the amygdala were studied. After delineating different individual amygdaloid nuclei,

immunoreactive neurons for c-Fos, Egr.1, and Arc were quantified and analysed for each nucleus.

Almost all nuclei showed a considerable increase in c-Fos-ir cells in the JS rats compared to the control rats. However, c-Fos expression was also considerably increased in the amygdala of CS rats compared to the control group. Immunocytochemical studies revealed a differential increase in c-Fos immunolabelled cells in the individual nuclei throughout the amygdaloid complex in the JS rats compared to the CS and control rats (Fig.12). In areas such as the medial amygdaloid nucleus (Me), posteromedial cortical amygdaloid area (PMCo), and the amygdalohippocampal transitional area (AHi), dense populations of c-Fos-ir cells were observed in juvenile stimulated rats.

The Me falls into four subdivisions; anterodorsal (MeAD), anteroventral (MeAV), posterodorsal (MePD), and posteroventral (MePV) medial amygdaloid nuclei. In contrast to MeAV, MePD, and MePV, which displayed significantly more c-Fos-ir cells in the JS rats than in the CS, MeAD showed no significant difference amongst the two stimulated groups. However, both stimulated groups displayed considerably more c-Fos-ir cells in MeAD than the control group did. The bed nucleus of the stria terminalis is also a part of the extended amygdala, which receives projections from the AOB. Here, an increase in c-Fos-ir cells in the medial division, the anterior part of the bed nucleus of the stria terminalis (BSTMA), in the JS was observed compared to CCS and control rats (Fig. 13). While the expression of c-Fos protein in the BSTMA in JS was stronger than in the CS, in the lateral division, the anterior part of the bed nucleus of the stria terminalis (BSTL), the differentiation was inverse, showing more c-Fos immunoreactive cells in the CS than in the JS rats.

Immunocytochemical studies indicated also a considerable increase in Egr.1-ir cells in the JS amygdala as compared to the CS and control groups. Increased Egr.1 immunoreactivity was observed throughout the rostrocaudal parts of the amygdala in the JS rats (Fig. 14). Arc immunoreactive cells such as PMCo and AHi were preferentially observed in the posterior parts of the amygdala. Here, the expression was high in JS compared to the two other groups (Fig.15). While many Arc-ir cells were displayed in the medial amygdala, especially in the MePD and MePV, of the JS group, these areas showed not significant difference among the three groups of rats.

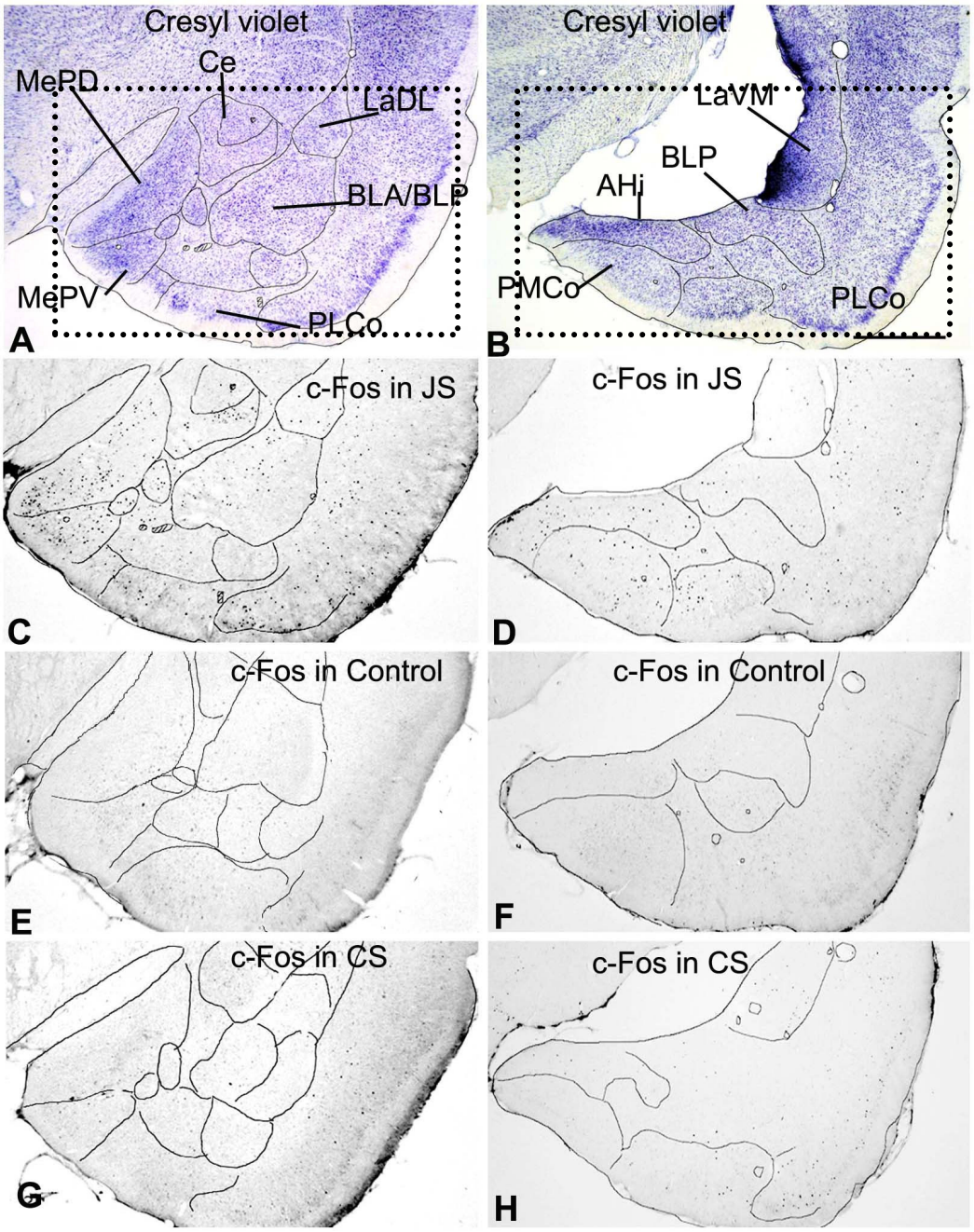


**Fig. 12 Expression of c-Fos in the amygdala in three groups of rats**

Medial parts of the amygdala, including the MePD, MePV, BLA, BLP and Ce (A), and the caudal part of amygdala, including the PMCo and AHi (B), are displayed in cresyl violet stained frontal sections. Section (A) is adjacent to immunostained section (C), and section (B) is adjacent to section (D). Areas identified by rectangles in (A) represent the topographic and cytoarchitectonic identical level for immunostained sections (C), (E) and (G), and the rectangle in (B) represents the identical level of sections displayed in (D), (F) and (H). Immunostained sections with antibody against c-Fos demonstrate considerably increased c-Fos-ir cells

in the medial amygdala of JS group, especially MePD and MePV (C), in comparison to the identical areas in the control (E) and CS (F) groups. Although few c-Fos-ir neurons were observed in the BLA, BLP, and PLCo of JS compared to MePD and MePV, the amount of these c-Fos positive cells was higher than the amount of immunoreactive neurons in the identical areas of the control and even CS group. In the posterior parts of the amygdala, considerably more c-Fos-ir cells were observed in the PMCo, AHi, and even PLCo of the JS group (D) in comparison to the control (F) and CS (H) groups. Only few c-Fos-ir neurons were observed in the identical nuclei in the CS and control groups. Scale bar 1000 µm.

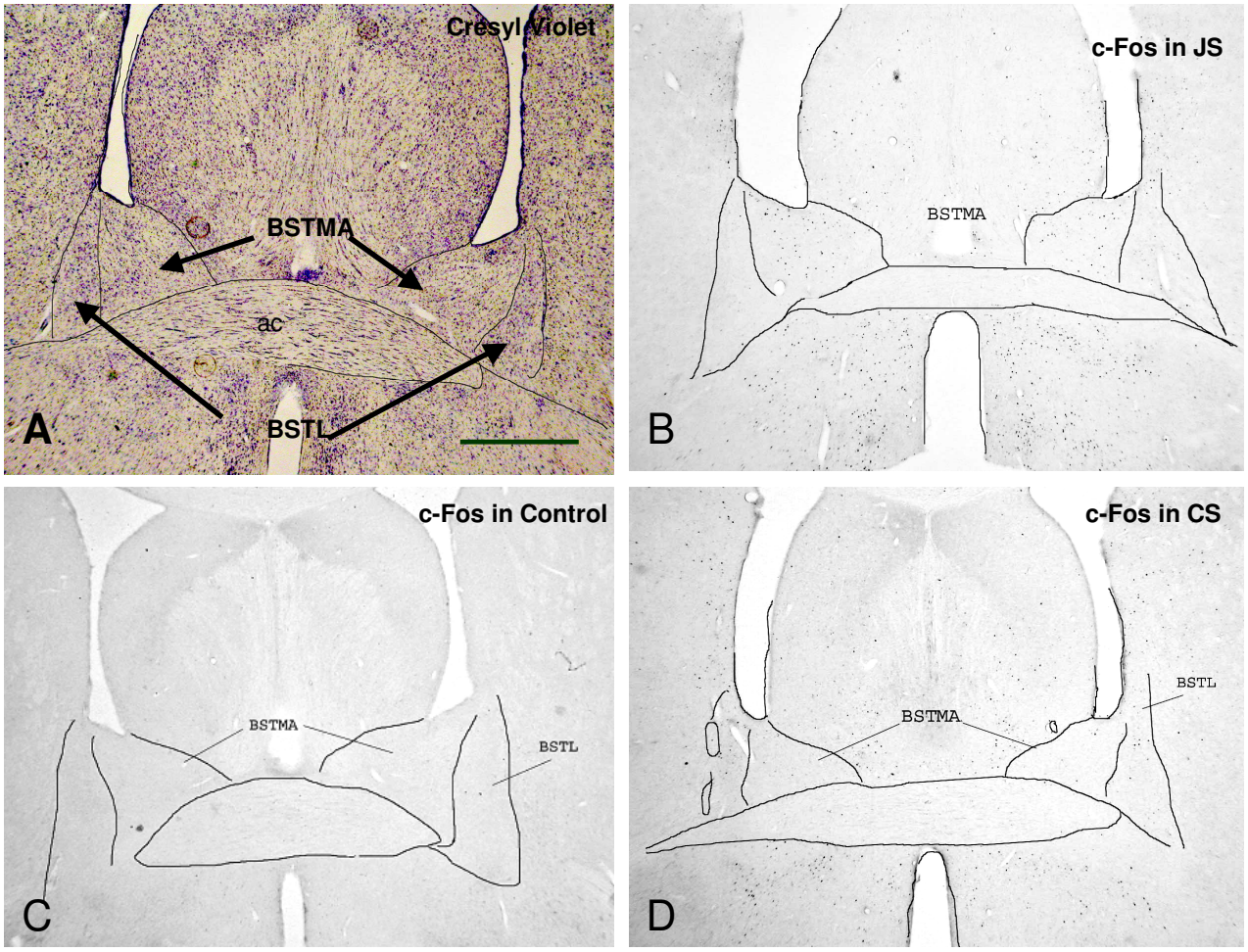


**Fig. 13 Expression of c-Fos in the BNST of three groups in rats**

Anteromedial (BSTMA) and anterolateral (BSTL) parts of the bed nucleus of the stria terminalis are indicated in cresyl violet stained coronal section (A). Juvenile stimulation caused considerable increase in c-Fos immunoreactive neurons in the BSTMA (B), while the lateral part, the BSTL, showed only few c-Fos-ir neurons. Both nuclei showed few positive signals in the control group (C). Although few c-Fos-ir cells were visualised in the BSTMA of the CS rats (D), considerably more c-Fos-ir cells were observed in the BSTL of the CS group. Scale bar 1000 µm.

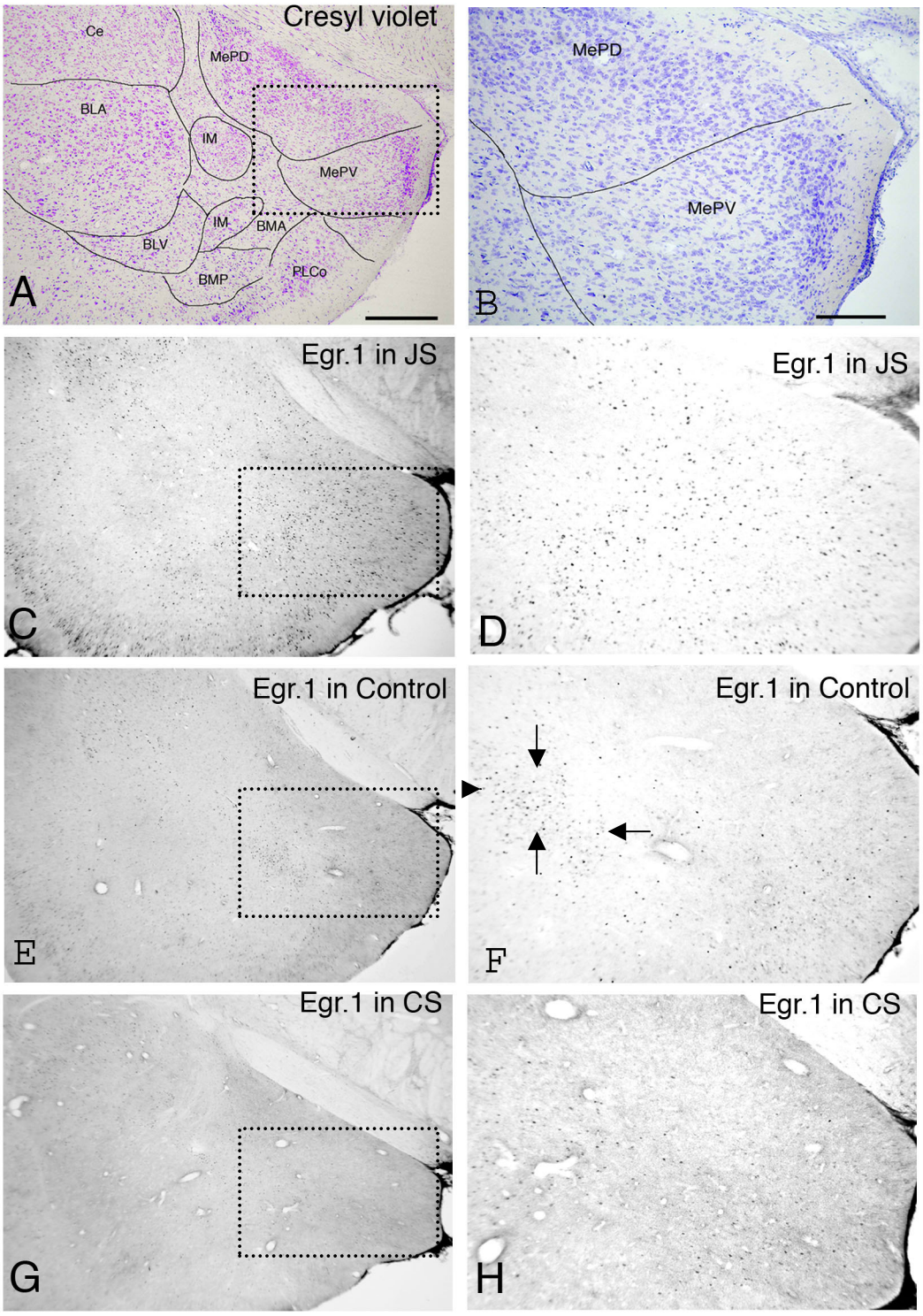


**Fig. 14 Egr.1 expression in the medial amygdaloid nucleus in three groups of rats**

A. Cresyl violet stained frontal section representing a medial level of the amygdala. This section contained individual nuclei such as Ce, BLA, BLV, BMP, BMA, IM, PLCo, MePD, and MePV. This section is adjacent to

immunostained section (C). Rectangles in the left column represent areas which are shown with higher magnification in the right column. Fig. B displays a higher magnified image of the MePD and MePV parts of the medial amygdaloid nucleus, which is identified by the rectangle in A. Juvenile stimulation caused many Egr.1 immunopositive neurons in the medial amygdala (C), but neither control (E) nor carvone stimulation (G) resulted in such an increase in Egr.1-ir cells in the identical regions. Highly magnified photomicrographs showed a considerable increase in Egr.1-ir cells in the MePD and MePV of JS (D) when compared to the control (F) and carvone stimulated rats. Although the intercalated mass cells nucleus displayed many Egr.1-ir cells in the control group (surrounded by arrowheads in F), only few immunopositive cells were visualised in the medial amygdala (F) of the control rats. Few Egr.1-ir cells were observed in the MePD and MePV of the carvone stimulated group (H). Scale bar 500 µm in A, 200 µm in B.

To simplify the analyses, the individual nuclei of the amygdala were categorised according to four functional systems: the olfactory amygdala, the vomeronasal amygdala, the autonomic amygdala, and the frontotemporal amygdala. Subsequently, the expression patterns of IEGs in these four systems were examined. The amygdalar olfactory system consists of the nucleus of the lateral olfactory tract (LOT), anterior cortical amygdaloid area (ACo), and posterolateral cortical amygdaloid nucleus (PLCo). Nuclei such as the bed nucleus of the accessory olfactory tract (BAOT), MeAD, MeAV, MePD, MePV, PMCo, and AHi constitute the vomeronasal amygdala. The lateral and basolateral nuclei form the frontotemporal amygdala, and the central nucleus belongs to the autonomic amygdala.

The analysis of the data revealed that all of the amygdalar functional systems except for the autonomic amygdala displayed more c-Fos-ir cells in the JS than in the control group (Fig. 16). The autonomic amygdala (containing the central amygdaloid nucleus) displayed no evidence of an increase in c-Fos-ir cells in the JS compared to the control rats. In the vomeronasal amygdala, a considerable increase in c-Fos-ir cells was observed in the JS rats compared to both the control and CS groups. The olfactory and frontotemporal amygdala showed no significant differences amongst the two stimulated groups, but the autonomic amygdala showed an increased Fos induction in the CD group compared to the JS and control groups. Among the four different amygdalar systems analysed, differential patterns of Egr.1 expression were observed in the three groups of rats (Fig. 17). A significantly increased number of Egr.1-ir neurons was observed in the vomeronasal and olfactory amygdala systems of the JS group when compared to the two other groups, namely the CS and control rats.

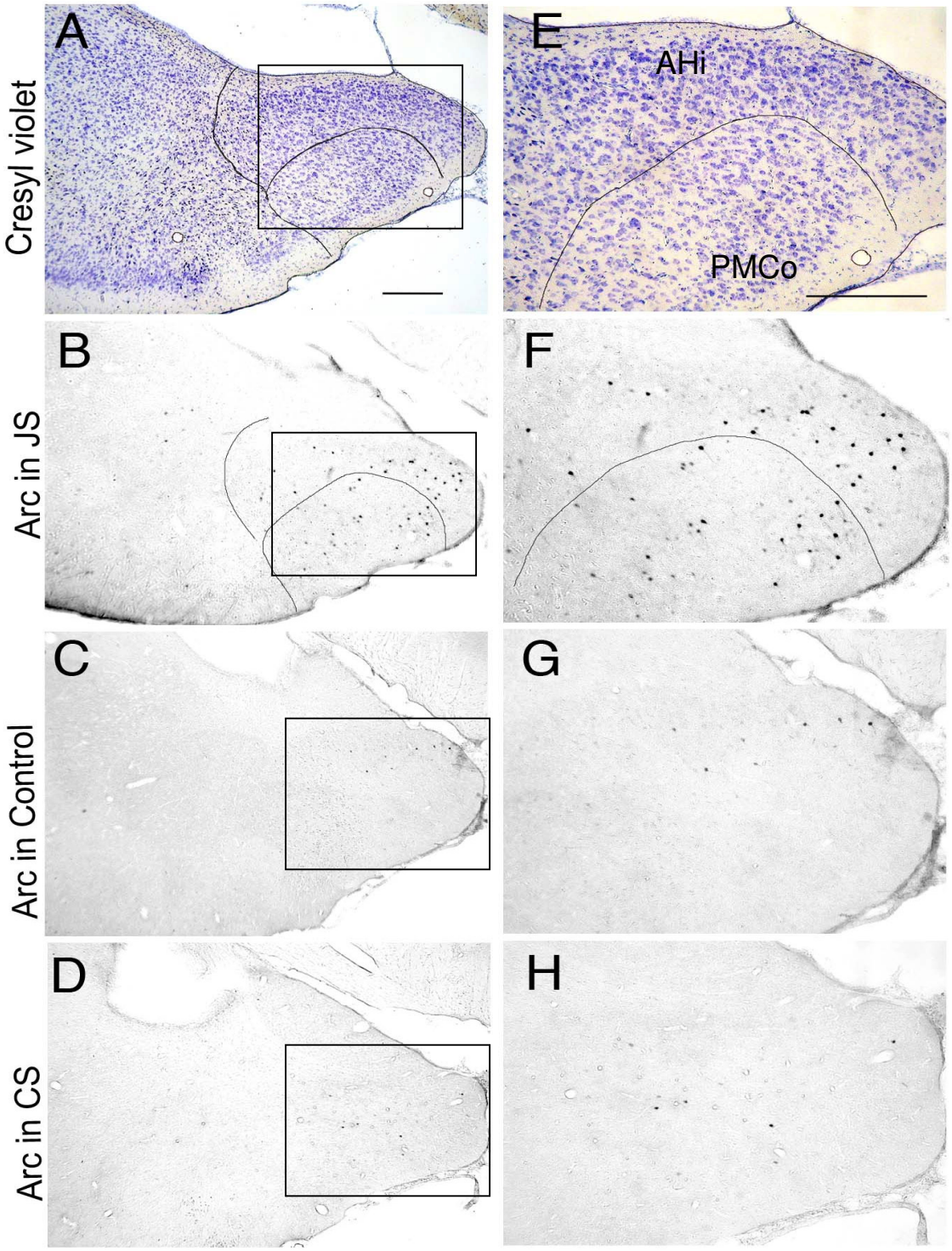


**Fig. 15 Expression of Arc in the amygdala of three groups of rats**

A. Cresyl violet stained frontal section representing a caudal level of the amygdala, including posteromedial cortical amygdaloid nucleus (PMCo) and amygdalohippocampal transitional area (AHi). This section is adjacent to immunostained section (B). Higher magnified photomicrograph (E) indicates the cytoarchitecture

of PMCo and AHi delineated by a rectangle in (A). Highly magnified photographs in the right column indicate areas identified by rectangles in the left column, and show considerably more Arc-Ir cells in the (AHi) and (PMCo) of the JS (F) compared to the control (G) and the carvone stimulated (H) rats. Few Arc-ir neurons were observed in the identical areas of the amygdala in CS and control rats. Scale bar 500 mm.

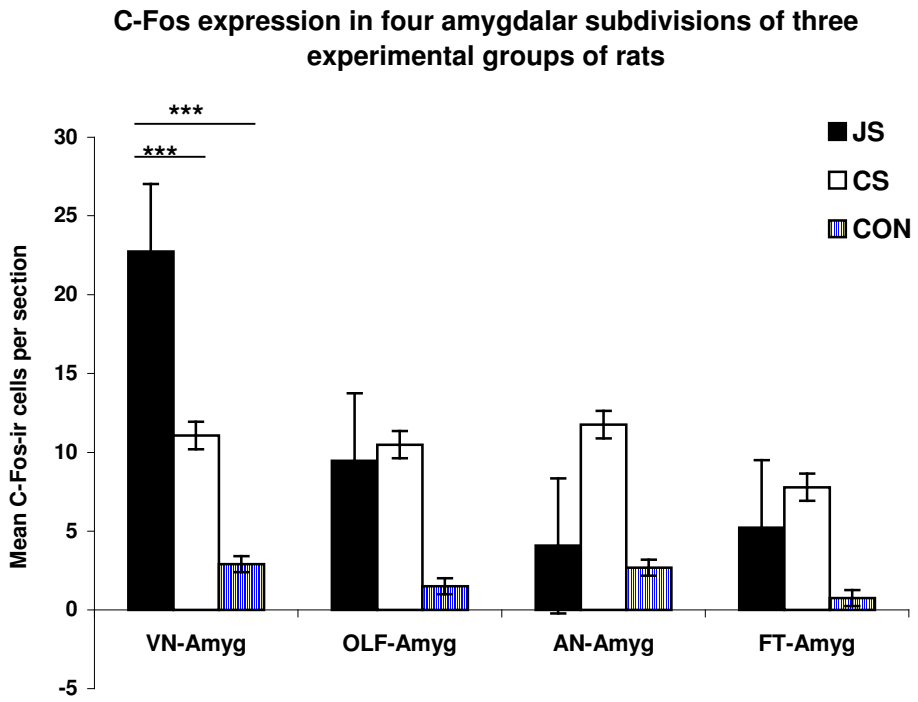


**Fig. 16 Fos expression in the four functional amygdalar subsystems in three groups of rats**

Histograms represent the mean (±S.E) numbers of c-Fos positive cells quantified in the four amygdaloid subsystems for the JS, CS, and control groups. Both juvenile and carvone stimulation significantly induced c-Fos expression in the amygdala. But the JS group displayed significantly more c-Fos-ir cells in the vomeronasal amygdala than the two other groups. While the olfactory and frontotemporal amygdala showed no significant differences between the two stimulated groups of JS and CS, the autonomic amygdala showed more Fos induction in the CS group than the JS and control groups did. Abbreviations: JS: juvenile stimulated group, CS: carvone stimulated group, VN-Amyg: vomeronasal amygdala, OLF-Amyg: olfactory amygdala, AN-Amyg: autonomic amygdala, FT-Amyg: frontotemporal amygdala.

Although there was no significant difference in Egr.1 immunoreactivity in the autonomic system between the three groups, the two groups of stimulated rats showed more Egr.1 immunolabelled cells in the frontotemporal system.

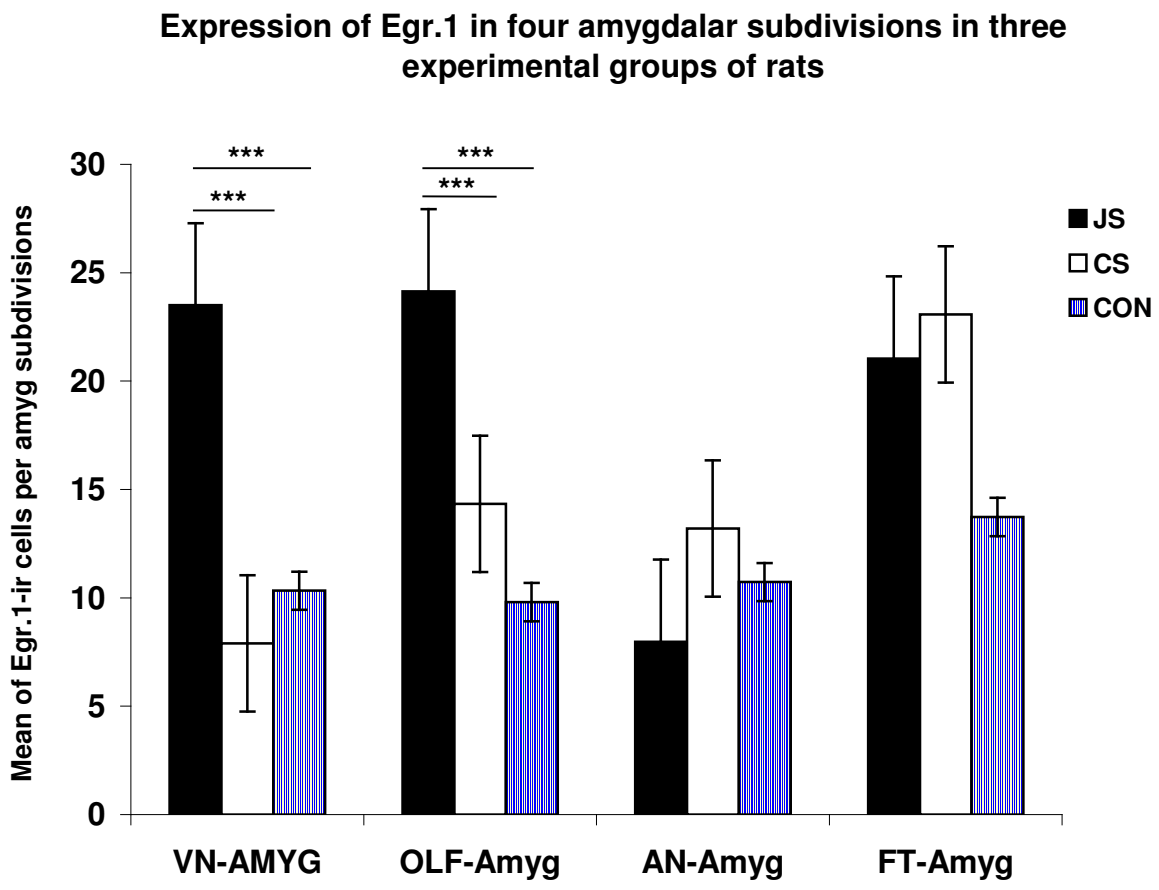


**Fig. 17 Egr.1 expression in the four different amygdalar subsystems in three groups of rats**
Histograms represent the mean (±S.E) numbers of Egr.1-ir neurons quantified in the four amygdalar functional systems of the JS, CS, and control group. Juvenile stimulation induced significantly more Egr.1 expression in the vomeronasal and olfactory amygdala of the JS group than in the two other groups. While both juvenile and carvone stimulation induced significantly more Egr.1 in the frontotemporal amygdala, the autonomic amygdala showed no significant differences among the three groups of rats. Abbreviations: AN-Amyg: autonomic amygdala, FT-Amyg: frontotemporal amygdala, OLF-Amyg: olfactory amygdala, VN-Amyg: vomeronasal amygdala.

To study the neuronal activation in individual nuclei during the social recognition process, the expression of c-Fos in the olfactory and vomeronasal systems of the amygdala were analysed in detail. Three subnuclei of the medial amygdaloid nucleus (MeAV, MePD, and MePV), as well as PMCo, AHi, and BSTMA displayed significantly more c-Fos in the JS group when compared to the CS and control rats (Fig. 18). None of the individual nuclei of the amygdalar olfactory system showed a significant difference between the two stimulated

groups of rats (detailed data are presented in Table 3.1). The analysis of the Egr.1 distribution in the individual nuclei of the amygdalar vomeronasal system revealed that many nuclei displayed more Egr.1-ir cells in the JS rats compared to the two other groups. However, all four subnuclei of the medial amygdaloid nucleus (MeAD, MeAV, MePD, and MePV) and PMCo displayed significantly more Egr.1 cells in the JS when compared to the CS and control rats (Fig. 19).

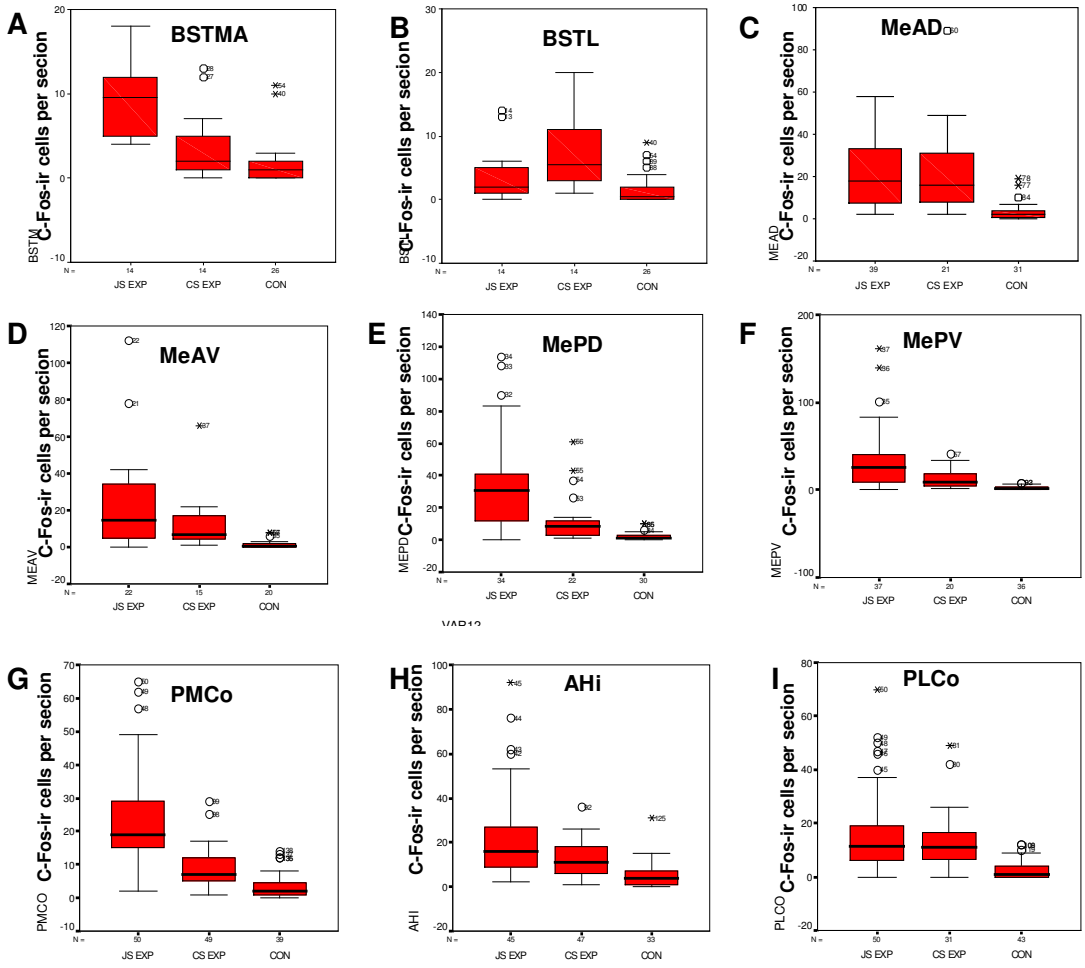


**Fig-18 Fos expression in individual nuclei of the VN-amygdala of three groups of rats**

Juvenile stimulation caused considerably increased c-Fos immunoreactivity in the individual nuclei in the vomeronasal amygdala of the JS rats compared to the CS and control rats. An increase in c-Fos-ir cells in the BSTMA was observed in the JS compared to the CS and control rats (A) while the adjacent area, BSTL, displayed more c-Fos immunoreactive cells in the CS than in the JS and control rats (B). While in MeAD and MeAV the pattern of Fos expression in the JS was similar to that in the CS, other medial amygdaloid

subnuclei like MePD, and MePV showed significantly higher c-Fos immunoreactivity in the JS than in the CS and control group. This pattern of increased immunoreactivity was also observed in the PMCo and AHi where many c-Fos-ir cells were observed in juvenile stimulated rats. In the olfactory amygdala, for example, in the PLCo (I), there was no significant difference in c-Fos immunoreactivity between the two stimulated groups.

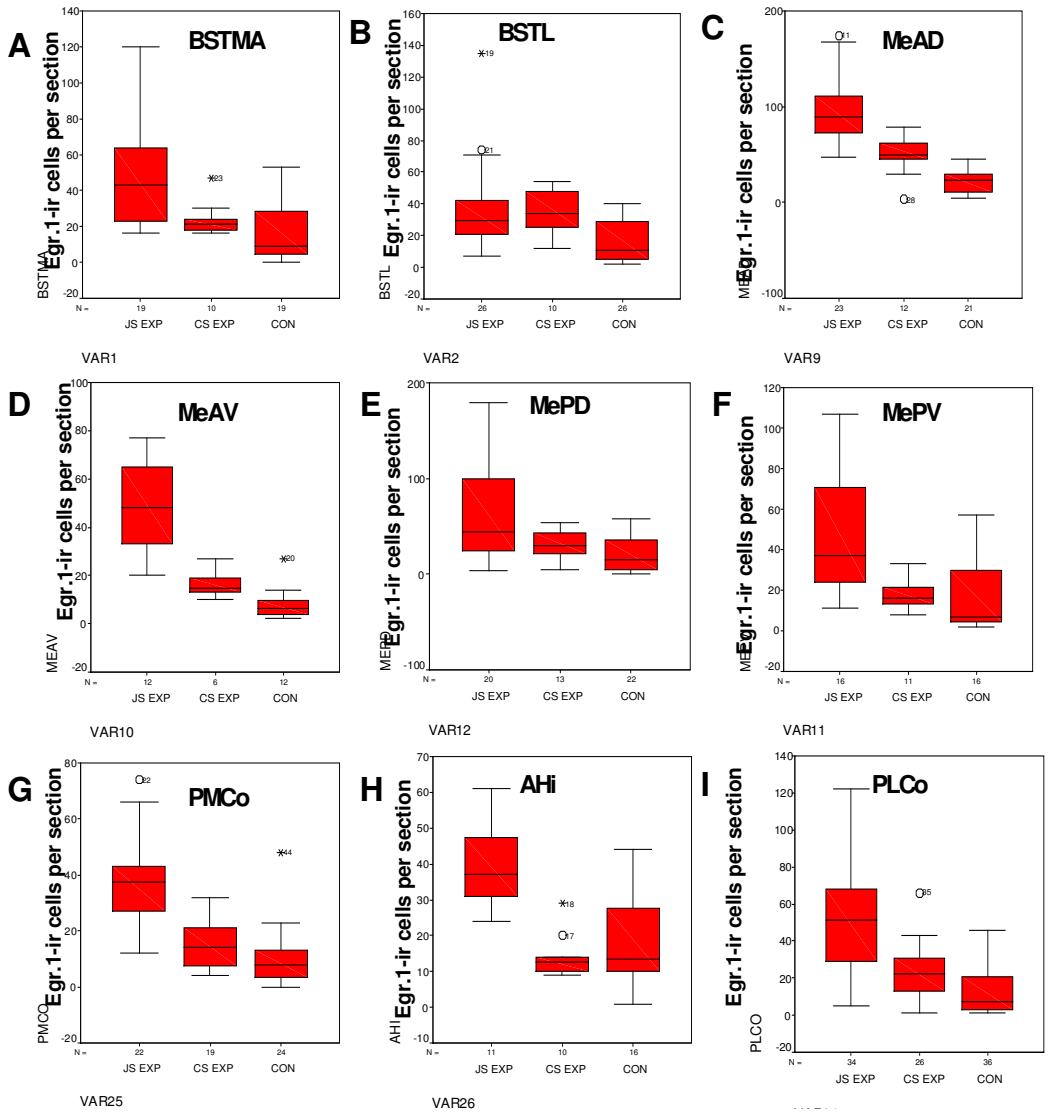


**Fig. 19 Egr.1 expression in the individual nuclei of the VN-amygdala in three groups of rats**

Juvenile stimulation caused considerably increased Egr.1 immunoreactivity in the amygdalar individual nuclei in the JS rats compared to the CS and control rats. A significant increase in Egr.1-ir cells was observed in the BSTMA in the JS compared to the CS and control rats (A) while the adjacent area, BSTL, did not displayed different patterns of Egr.1 expression in the three groups of rats (B). Compared to the other two groups, juvenile stimulation induced significantly more Egr.1 in many of the individual nuclei of the VN-amygdala, such as MeAD, MeAV, MePD, MePV, PMCo, and AHi. Even in some individual nuclei in the amygdalar

olfactory system, such as PLCo, Egr.1 immunoreactive cells were significantly increased in the JS compared to the CS and control groups.

**Table 3.1 Summary of total, average, maximum, minimum, standard deviation and Mann-Whitney test results in the individual amygdalar subnuclei for c-Fos expression in three groups of rats**

| Area / Statistic | BSTMA | BSTL | BSTIA | BAOT | MEAD | MeAV | MePV | MePD | PMCo | AHI | LOT | ACO | BMA | BLV | BLP | BMP | IM | PLCo | Ce | BLA | LaDL | LaVM | LaVL |
|---|---|---|---|---|---|---|---|---|---|---|---|---|---|---|---|---|---|---|---|---|---|---|---|
| SUM JS | 132 | 56 | 63 | 169 | 815 | 497 | 1268 | 1167 | 1183 | 1034 | 475 | 907 | 628 | 78 | 197 | 234 | 215 | 806 | 219 | 401 | 124 | 553 | 64 |
| SUM CS | 52 | 107 | 46 | 137 | 391 | 150 | 257 | 287 | 436 | 575 | 398 | 977 | 354 | 50 | 151 | 117 | 109 | 424 | 447 | 402 | 106 | 551 | 32 |
| SUM Con | 27 | 29 | | 3 | 60 | 9 | 54 | 66 | 106 | 116 | 9 | 70 | 90 | 25 | 35 | 22 | 27 | 66 | 101 | 60 | 16 | 26 | 9 |
| Mean JS | 9,43 | 4 | 9 | 7,358 | 20,9 | 22,59 | 34,27 | 34,32 | 23,66 | 22,98 | 20,65 | 16,49 | 9,968 | 2 | 3,229 | 5,087 | 5,8 | 16,12 | 4,1 | 5,6 | 2,2 | 8,64 | 2,13 |
| Mean CS | 3,71 | 7,64 | 9,2 | 9.79 | 18.62 | 10 | 12,85 | 13,04 | 8,9 | 12,23 | 13,72 | 22,20 | 9,316 | 2,174 | 4,194 | 4,33 | 6,05 | 13,68 | 12 | 8,4 | 3,3 | 12,8 | 1,88 |
| Mean Con | 2,25 | 2,42 | | 0,27 | 3,33 | 0,9 | 1,8 | 2,54 | 4,61 | 5,8 | 0,75 | 1,842 | 2,25 | 0,714 | 0,972 | 0,846 | 1,7 | 2,357 | 2,7 | 1,3 | 0,4 | 0,70 | 0,41 |
| Max JS | 18 | 14 | 18 | 20 | 58 | 112 | 161 | 114 | 65 | 92 | 62 | 58 | 46 | 15 | 11 | 26 | 27 | 70 | 34 | 38 | 11 | 36 | 10 |
| Max CS | 13 | 20 | 17 | 31 | 57 | 21 | 41 | 61 | 29 | 36 | 46 | 78 | 40 | 9 | 19 | 18 | 17 | 49 | 40 | 41 | 21 | 56 | 5 |
| Max Con | 10 | 9 | 0 | 1 | 19 | 3 | 8 | 10 | 14 | 31 | 2 | 10 | 29 | 5 | 6 | 5 | 14 | 12 | 37 | 7 | 3 | 4 | 2 |
| Min JS | 4 | 0 | 4 | 0 | 2 | 0 | 0 | 0 | 2 | 2 | 0 | 0 | 0 | 0 | 0 | 0 | 0 | 0 | 0 | 0 | 0 | 0 | 0 |
| Min CS | 0 | 1 | 5 | 1 | 2 | 1 | 1 | 1 | 1 | 1 | 0 | 0 | 1 | 0 | 0 | 0 | 0 | 0 | 0 | 0 | 0 | 0 | 0 |
| Min Con | 0 | 0 | 0 | 0 | 0 | 0 | 0 | 0 | 0 | 0 | 0 | 0 | 0 | 0 | 0 | 0 | 0 | 0 | 0 | 0 | 0 | 0 | 0 |
| SDEV JS | 4,685 | 4,35 | 4,62 | 9.63 | 13 | 7.8 | 36,3 | 30,37 | 14,77 | 20,2 | 21,90 | 14,31 | 8,91 | 2,77 | 3,0 | 5,3 | 5,9 | 15,6 | 5,3 | 7,8 | 2,9 | 8,71 | 2,583 |
| SDEV CS | 4,27 | 5,47 | 4,7 | 9,8 | 20,4 | 16,3 | 10,95 | 15,3 | 5,77 | 8,0 | 13,2 | 17,67 | 9,57 | 2,348 | 4,055 | 3,980 | 5,03 | 10,71 | 11 | 8,8 | 4,2 | 13,65 | 1,691 |
| SDEV Con | 2,6 | 2,87 | | 0,467 | 5,41 | 1,1 | 2,0 | 2,7 | 4,3 | 7,1 | 0,75 | 2,6 | 5,2 | 1,3 | 1,3 | 1,2 | 3,5 | 3,26 | 5,9 | 1,7 | 0,7 | 1,024 | 0,666 |
| JS&CS | 0,002 | 0,024 | | 0,676 | 0,466 | 0,225 | 0,004 | 0,001 | 0,001 | 0,004 | 0,396 | 0,094 | 0,378 | 0,586 | 0,237 | 0,872 | 0,67 | 0,965 | 0,000 | 0,036 | 0,160 | 0,202 | 0,856 |
| JS&Con | 0,001 | 0,252 | | 0,001 | 0,001 | 0,001 | 0,001 | 0,001 | 0,001 | 0,001 | 0,001 | 0,001 | 0,001 | 0,003 | 0,001 | 0,001 | 0,001 | 0,001 | 0,018 | 0,000 | 0,000 | 0,001 | 0,001 |
| CS&Con | 0,631 | 0,004 | | 0,001 | 0,001 | 0,001 | 0,001 | 0,001 | 0,001 | 0,001 | 0,001 | 0,001 | 0,001 | 0,002 | 0,001 | 0,001 | 0,001 | 0,001 | 0,000 | 0,000 | 0,000 | 0,001 | 0,002 |

Table 3.1 represents detailed data of c-Fos expression in the individual nuclei of the amygdala in three groups of rats. The quantified c-Fos-ir cells in each group (SUM), the average (Mean) of immunoreactive cell per section, standard deviation (SDEV), and Mann-Whitney test results which compared the data of c-Fos immunopositive cells in different individual nuclei of the amygdala between each two groups, JS versus CS, JS versus control and CS versus control.

**Table 3.2 Summary of total, average, maximum, minimum, standard deviation and Mann-Whitney test results in the individual amygdalar nuclei for Egr.1 expression in three group of rats**

| Data \ Area | BSTMA | BSTL | BSTIA | BAOT | MEAD | MeAV | MePV | MePD | PMCO | AHI | LOT | ACO | BMA | BLV | BLP | BMP | IM | PLCO | Ce | BLA | LaDL | LaVM | LaVL |
|---|---|---|---|---|---|---|---|---|---|---|---|---|---|---|---|---|---|---|---|---|---|---|---|
| Sum JS | 244 | 140 | 31 | 198 | 1005 | 403 | 988 | 976 | 1063 | 618 | 1941 | 2244 | 1922 | 165 | 139 | 387 | 624 | 1076 | 351 | 406 | 2473 | 980 | 76 |
| Sum CS | 50 | 43 | 13 | 76 | 425 | 163 | 252 | 240 | 189 | 164 | 1459 | 1060 | 663 | 115 | 101 | 145 | 487 | 345 | 568 | 479 | 2474 | 954 | 50 |
| Sum Con | 90 | 65 | 26 | 28 | 300 | 89 | 250 | 290 | 270 | 308 | 75 | 347 | 667 | 79 | 109 | 183 | 464 | 323 | 322 | 306 | 1109 | 623 | 104 |
| Mean JS | 13,6 | 7,78 | 7,75 | 9 | 31,4 | 19,2 | 36,59 | 37,5 | 25,9 | 19,3 | 64,7 | 40,8 | 28,3 | 3,9 | 3,48 | 10,2 | 16 | 26,9 | 7,98 | 7,52 | 38 | 19,6 | 4,222 |
| Mean CS | 3,13 | 2,69 | 6,5 | 6,33 | 16,3 | 9,59 | 10,5 | 10,9 | 5,25 | 4,97 | 48,6 | 19,6 | 13,5 | 3,3 | 2,81 | 4,14 | 14,8 | 10,5 | 13,2 | 8,71 | 43,4 | 22,2 | 3,125 |
| Mean Con | 7,5 | 5,42 | 8,67 | 3,5 | 18,8 | 8,9 | 9,615 | 10,7 | 9,31 | 13,4 | 6,25 | 15,8 | 20,2 | 2,4 | 2,95 | 5,55 | 20,2 | 8,97 | 10,7 | 6,95 | 23,6 | 14,2 | 4,952 |
| Max JS | 42 | 26 | 11 | 34 | 92 | 49 | 85 | 105 | 95 | 90 | 152 | 123 | 74 | 16 | 24 | 42 | 54 | 75 | 26 | 40 | 155 | 55 | 14 |
| Max CS | 11 | 14 | 9 | 17 | 59 | 36 | 34 | 33 | 16 | 20 | 246 | 80 | 44 | 24 | 11 | 25 | 53 | 46 | 54 | 58 | 140 | 122 | 11 |
| Max Con | 12 | 13 | 11 | 6 | 67 | 28 | 33 | 42 | 29 | 46 | 14 | 36 | 43 | 5 | 19 | 19 | 49 | 34 | 32 | 32 | 121 | 67 | 11 |
| Min JS | 0 | 0 | 2 | 0 | 5 | 5 | 3 | 3 | 6 | 1 | 10 | 2 | 2 | 0 | 0 | 1 | 2 | 1 | 0 | 0 | 4 | 1 | 0 |
| Min CS | 0 | 0 | 4 | 0 | 1 | 1 | 0 | 0 | 0 | 0 | 2 | 0 | 1 | 0 | 0 | 0 | 1 | 0 | 0 | 0 | 1 | 1 | 0 |
| Min Con | 1 | 0 | 7 | 0 | 7 | 0 | 1 | 0 | 1 | 0 | 0 | 1 | 3 | 0 | 0 | 1 | 3 | 1 | 0 | 0 | 3 | 0 | 0 |
| SDEV JS | 10,9 | 7,7 | 4,27 | 8,43 | 16,7 | 11,6 | 24,85 | 25,9 | 20,3 | 18,6 | 36,3 | 24,7 | 19,6 | 3,8 | 4,76 | 8,79 | 12,1 | 20,7 | 6,29 | 6,79 | 29,6 | 14,7 | 4,008 |
| SDEV CS | 3,48 | 3,2 | 3,54 | 4,72 | 12,9 | 10,3 | 10,24 | 10,3 | 4,58 | 5,04 | 58,6 | 17,1 | 11,4 | 4,5 | 3,06 | 4,93 | 12,3 | 11,7 | 13,1 | 9,82 | 31,3 | 22,8 | 3,481 |
| SDEV Con | 3,4 | 4,21 | 2,08 | 2,73 | 14,4 | 9,87 | 10,28 | 10,4 | 8,89 | 12,6 | 3,62 | 8,83 | 11,8 | 1,9 | 3,9 | 4,06 | 14,4 | 8,31 | 8,65 | 7,89 | 22,9 | 15,4 | 2,729 |
| JS&CS | 0.000 | 0.03 | 0.8 | 0.71 | 0.000 | 0.002 | 0.000 | 0.000 | 0.000 | 0.000 | 0.005 | 0.000 | 0.000 | 0.205 | 0.57 | 0.000 | 0.54 | 0.000 | 0.11 | 0.9 | 0.30 | 0.76 | 0.86 |
| JS&Con | 0.17 | 0.79 | 0.9 | 0.12 | 0.001 | 0.009 | 0.000 | 0.000 | 0.000 | 0.18 | 0.000 | 0.000 | 0.09 | 0.17 | 0.62 | 0.014 | 0.36 | 0.000 | 0.27 | 0.145 | 0.001 | 0.03 | 0.25 |
| CS&Con | 0.004 | 0.03 | 0.8 | 0.305 | 0.508 | 0.863 | 0.514 | 0.98 | 0.096 | 0.01 | 0.000 | 0.74 | 0.007 | 0.84 | 0.82 | 0.04 | 0.21 | 0.96 | 0.78 | 0.18 | 0.000 | 0.05 | 0.13 |

Table 3.2 represents detailed data of Egr.1 expression in the individual nuclei of the amygdala in three groups of rats. The quantified c-Fos-ir cells in each group (SUM), the average (Mean) of immunoreactive cell per section, standard deviation (SDEV), and Mann-Whitney test results which compared the data of c-Fos immunopositive cells in different individual nuclei of the amygdala between each two groups, JS versus CS, JS versus control and CS versus control.

## 5. The mRNAs encoding for GAD65 and GAD67, vesicular glutamate transporters 1 and 2, are heterogeneously expressed in the rat amygdala

In order to investigate the co-expression of c-Fos with glutamic acid decarboxylase (GAD) and/or vesicular glutamate transporters, the distribution of mRNAs that encode these proteins were studied in the amygdala.

### 5.1 Distribution of glutamic acid decarboxylase 65 and 67 mRNAs in the amygdala

The mRNAs of two isoforms of glutamic acid decarboxylase, GAD65 and GAD67, were localised in the amygdaloid complex of the rat by in situ hybridisation (Fig. 20 C and D, respectively). While in most of the labelled subnuclei the frequency of labelled cells was similar for the two GAD mRNAs, there was some heterogeneity in the intensity of labelling among the neuronal populations.

In many amygdalar regions, such as BLA, LADL, ACo, PLCo, and BMA, the patterns of labelling were similar for both GAD mRNAs. In some areas, such as IM and Ce, the density of labelling for GAD67 mRNA was higher than that for GAD65 mRNA. The intensity of labelling in the amygdala was different for the two GAD mRNAs. Some cells were heavily labelled while others were weakly labelled. The intensity of labelling for GAD65 was higher than that for GAD67, especially in the medial amygdaloid nucleus. The pattern of labelling for GAD65 mRNA in the medial amygdala was heterogeneous. This area of the amygdala showed strong labelling for both GAD mRNAs. Numerous neurons in the posterodorsal and anterodorsal medial amygdala were moderately to strongly labelled for GAD65 mRNA. GAD65 mRNA containing neurons in the ventral parts of the medial amygdala were labelled mildly and were less dense. In the AHi and PMCo, numerous cells were labelled for GAD65 mRNA.

The same expression pattern was observed for GAD67 mRNA. While the lateral, basal and basolateral parts of the amygdala were homogenously and strongly labelled for GAD67 mRNA, the medial amygdala showed a dense but heterogeneous pattern of GAD67 mRNA labelled neurons. MeAD and MePD showed heterogeneous clusters of neurons densely labelled for GAD67 mRNA. By contrast, in the ventral parts of the medial amygdala, the neurons were less densely but homogeneously labelled. Numerous moderately to strongly labelled neurons were seen in the MePD, which were concentrated especially in the medial part of the MePD (MePDm). By contrast, in MePV, neurons expressing GAD67 mRNA were packed less dense. A dense population of neurons was moderately labelled for GAD67 mRNA in the intercalated cell mass nucleus. In the ACo, some less dense and mildly stained neurons were found while strongly labelled, scattered neurons were

observed in the PLCo, BMA, and BLA. In the central amygdala, densely packed neurons were stained mildly to strongly for GAD67 mRNA.

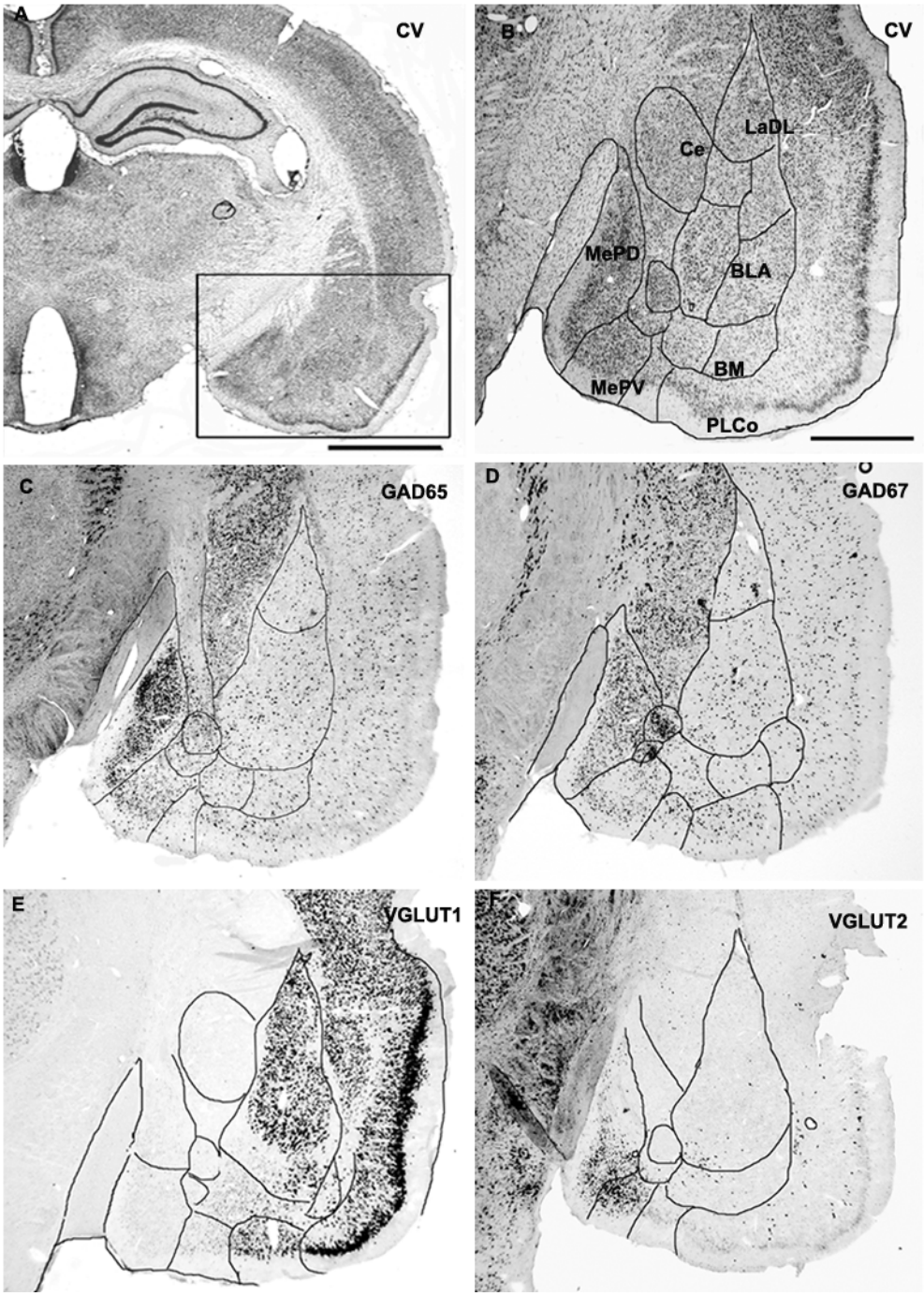


**Fig. 20 Comparative distribution patterns of GAD65, GAD67, vGLUT2, and vGLUT1 mRNA at the level of medial amygdala**

The cresyl violet staining coronal section of the rat brain shows the medial level of amygdala (A and B). Figures C and D are adjacent sections illustrating the localisation of GAD65 and GAD67 signal in rat amygdala, respectively. The medial amygdaloid nucleus displayed strong labelling for both GAD65 (C) and 67 (D) mRNAs whereas the expression of these mRNAs in lateral nuclei of the amygdala is much less than in medial nuclei. Figures E and F are adjacent sections illustrating the localisation of vGLUT1 and vGLUT2 signal in rat amygdala, respectively. VGLUT2 mRNA is expressed throughout the medial nuclei, whereas the expression of this mRNA in lateral nuclei of the amygdala is much less than in medial nuclei and only scattered cells are positive. But vGLUT1 is strongly labelled in the lateral amygdala while the medial amygdala is completely devoid of it. Scale bar 2 mm in (A), 1000 µm in B.

## 5.2 Distribution of vGLUT1 and vGLUT 2 mRNAs in amygdala

In situ hybridisation studies indicated that vGLUT1 is the predominant vesicular glutamate transporter in many of the amygdalar subnuclei (Fig. 20 E). Expression of vGLUT1 was observed at almost all levels of the amygdala, except for the BNST and the MeA subnuclei. In the anterior amygdaloid area, including AA, ACo, and the rostral part of BMA, only very few vGLUT1 mRNA positive neurons were detected. The LOT nucleus was found to express the highest level of vGLUT1 mRNA compared to the other amygdaloid nuclei analysed. Neurons within the LOT nucleus displayed a remarkably high vGLUT1 mRNA expression, together with a moderate expression of vGLUT2 mRNA.

High-intensity expression of vGLUT1 was also seen in the basolateral (BLA, BLV, and BLP) and lateral (LaDL, LaVL, and LaVM) nuclei. In the basomedial amygdaloid nucleus, the expression of vGLUT1 mRNA was weak in the rostral parts while a considerably strong expression was evident in its posterior parts. In the posterior amygdala (PMCo and AHi), numerous neurons strongly expressing vGLUT1 mRNA were seen. In the medial amygdala, only very few scattered and weakly labelled vGLUT1 mRNA expressing neurons were found in the Me.

Only few neurons labelled for vGUT2 mRNA were observed in the ACo, BAOT, BSTMP, BMA, IM, and PLCo nuclei. Neurons expressing vVGUT2 mRNA were also detected in the LOT. The BSTL and BLA nuclei were characterised by a lack of vGLUT2 mRNA expression, and the anterior BNST showed only few vGLUT2 mRNA labelled neurons.

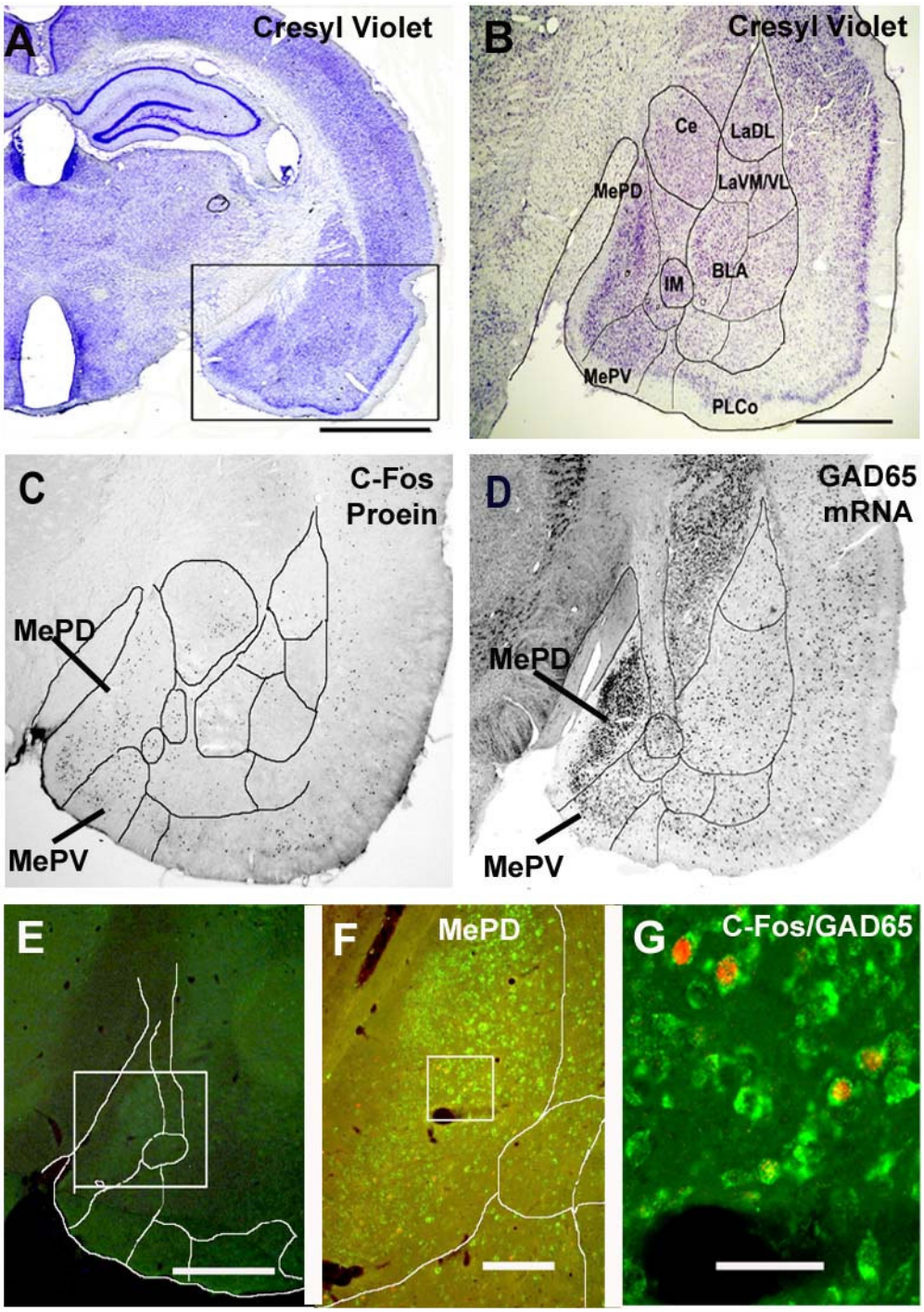


**Fig. 21 Co-expression of c-Fos and GAD65 mRNA in the posterodorsal medial amygdaloid nucleus (MePD) in the JS group of rats**

(A) and (B) present cresyl violet stained coronal sections of the rat brain containing amygdalar subnuclei. Fos expression pattern at the medial level of the amygdala of the JS group as displayed in a coronal section (C); in an adjacent section, the expression of GAD65 mRNA was observed in the MePD (D). Low power magnification image of GAD65 mRNA and c-Fos demonstrate the area of study (E). The boxed area in (E) is

higher magnified in (F). High-power micrograph of c-Fos protein and GAD65 mRNA demonstrates a co-expression in the MePD (G). Many c-Fos-ir cell contain GAD65 mRNA. Location of (G) is illustrated by the quadrangle in (F). Scale bar 2 mm in (A); 1 mm in (B and E); 200 µm in (F) and 50 µm in (G).

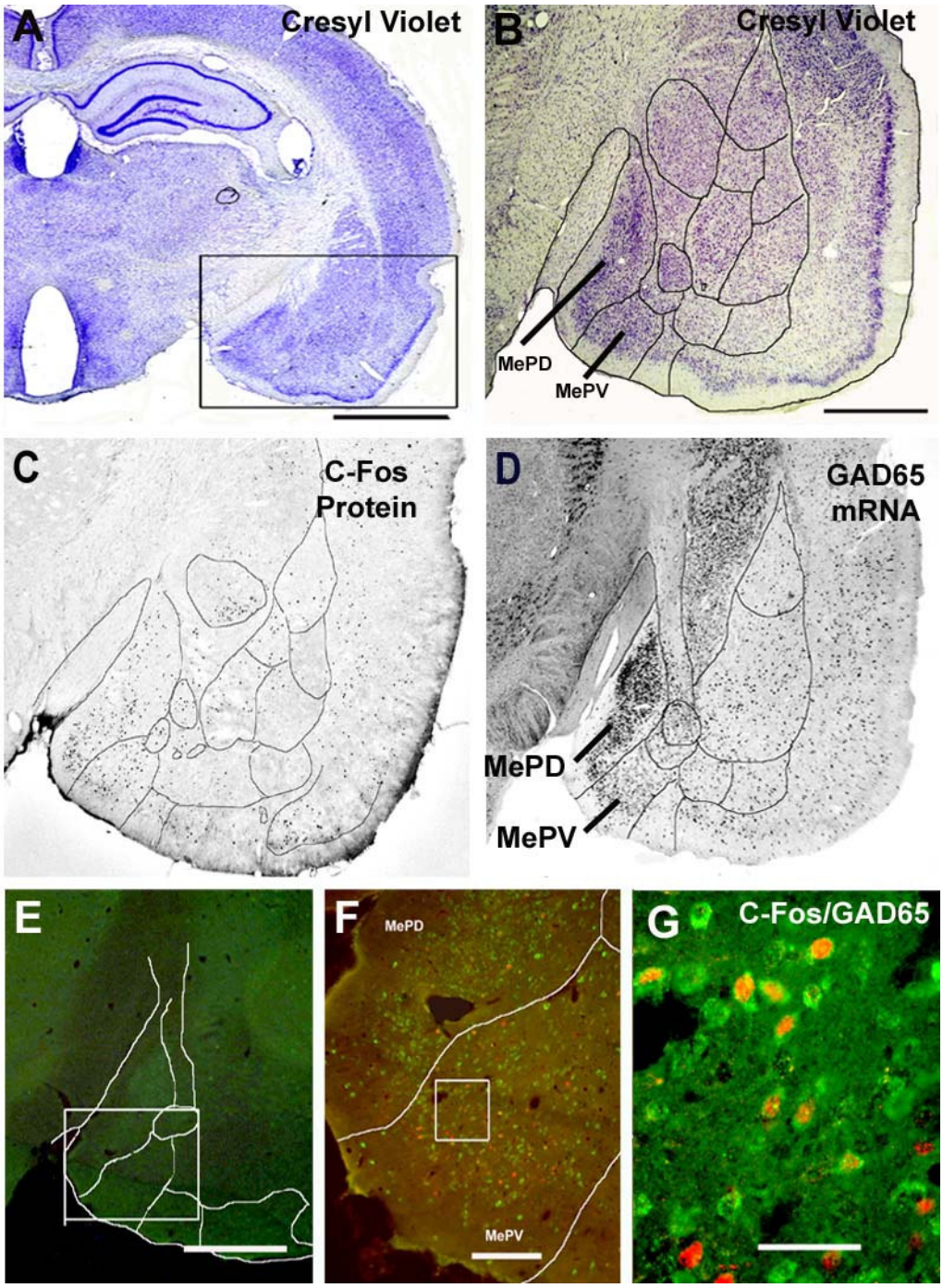


**Fig. 22 Co-expression of c-Fos and GAD65 mRNA in the posteroventral medial amygdaloid nucleus (MePV) in the JS group of rats**

(A) and (B) present cresyl violet stained coronal sections of the rat brain containing amygdalar subnuclei. Fos expression pattern at the medial level of the amygdala of the JS group as displayed in a coronal section (C); in an adjacent section, the expression of GAD65 mRNA was observed in the MePV (D). Low power magnification image of GAD65 mRNA and c-Fos demonstrate the area of study (E). The boxed area in (E) is higher magnified in (F). High-power micrograph of c-Fos protein and GAD65 mRNA demonstrates a co-expression in the MePV (G). Many c-Fos-ir cell contain GAD65 mRNA. Location of (G) is illustrated by the quadrangle in (F). Scale bar 2 mm in (A); 1 mm in (B and E); 200 µm in (F) and 50 µm in (G).

A considerably strong expression of vGLUT2 mRNA was observed throughout the medial amygdaloid nuclei, including the MeAD, MeAV, MePD, and MePV nuclei (Fig. 20 F). The MeA nucleus was characterised by a moderate to high expression of vGLUT2 mRNA. In contrast to many moderately labelled neurons in the MePV and MePDm, the lateral and intermediate parts of MePD expressed only few scattered vGLUT2 mRNA. Furthermore, numerous neurons strongly expressing vGLUT2 mRNA were detected in the PMCo and AHi nuclei. The PMCo and AHi individual nuclei expressed both vGLUT1 and 2 mRNAs. However, the medial and the lateral amygdala, together with basolateral amygdalar nuclei, exhibited a complementary distribution of the mRNAs that encode the vGLUT1 and vGLUT2 mRNAs.

### 6. Co-expression of c-Fos with GADs and vesicular glutamate transporters in the amygdala of the JS group

To study whether the neurons which were specifically activated by social stimulation may give rise to excitatory projections to further target areas or whether they may represent local inhibitory interneurons, the GABAergic or glutamatergic nature of the c-Fos-ir cells was determined. For this purpose, a combination of in situ hybridisation and immuno-cytochemistry was used. Thus, the expression of probes for glutamate decarboxylase 65 and 67 and probes for vesicular glutamate transporters vGLUT1 and vGLUT2 were detected by in situ hybridisation while c-Fos was detected by immunocytochemistry. Accordingly, the medial amygdala contained numerous neurons labelled for GAD65, GAD67, and vGLUT2 mRNAs. By contrast, only a few scattered neurons expressing vGLUT1 mRNA were detected in the Me. Numerous vGLUT1-expressing neurons were detected in the PMCo and AHi. In these regions, the c-Fos expression was significantly

increased in the juvenile stimulated rats compared to the control and carvone stimulated groups. For the quantification of the double labelling experiments, the amygdala regions MePD, MePV and PMCo were chosen. Robustly labelled cells only were included in the analysis.

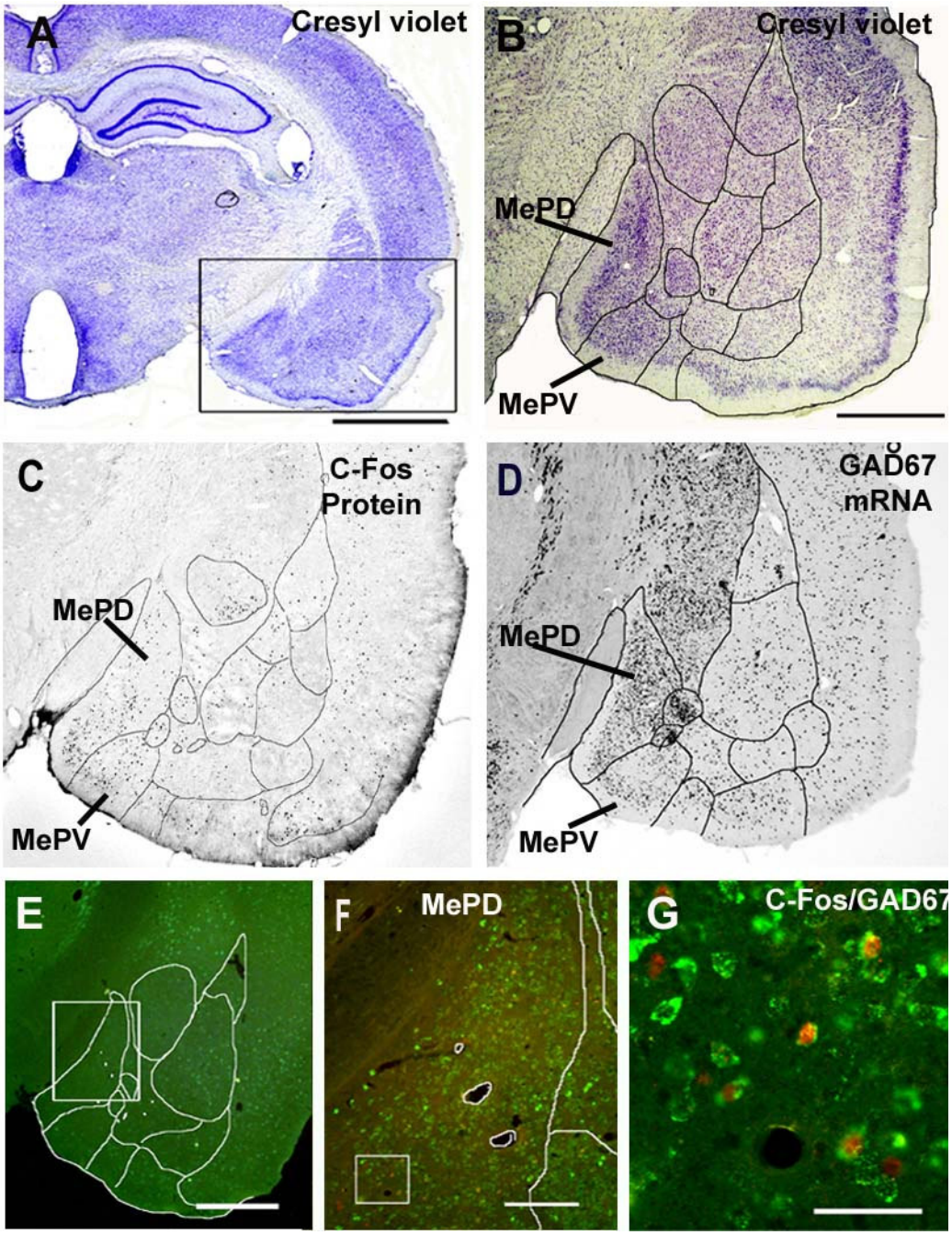


**Fig. 23 Co-expression of c-Fos and GAD67 mRNA in the posterodorsal medial amygdaloid nucleus (MePD) in the JS group of rats**

(A) and (B) present cresyl violet stained coronal sections of the rat brain containing amygdalar subnuclei. Fos expression pattern at the medial level of the amygdala of the JS group as displayed in a coronal section (C); in an adjacent section, the expression of GAD67 mRNA was observed in the MePD (D). Low power magnification image of GAD67 mRNA and c-Fos demonstrate the area of study (E). The boxed area in (E) is higher magnified in (F). High-power micrograph of c-Fos protein and GAD67 mRNA demonstrates a co-expression in the MePD (G). Many c-Fos-ir cell contain GAD67 mRNA. Location of (G) is illustrated by the quadrangle in (F). Scale bar 2 mm in (A); 1 mm in (B and E); 200 µm in (F) and 50 µm in (G).

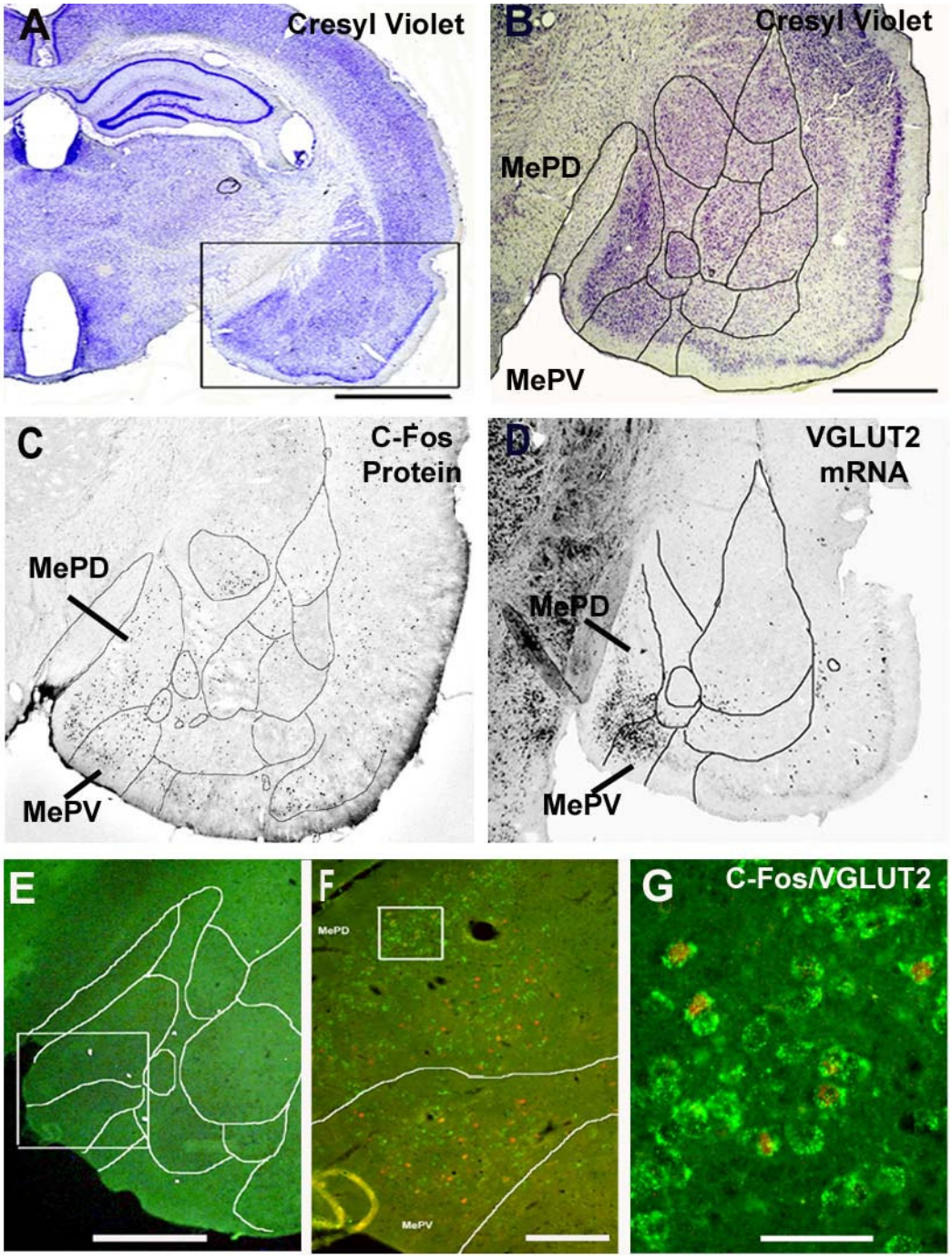

**Fig. 24 Co-expression of c-Fos and vGLUT2 mRNA in the posterodorsal medial amygdaloid nucleus (MePD) in the JS group of rats**

(A) and (B) present cresyl violet stained coronal sections of the rat brain containing amygdalar subnuclei. Fos expression pattern at the medial level of the amygdala of the JS group as displayed in a coronal section (C); in an adjacent section, the expression of vGLUT2 mRNA was observed in the MePD (D). Low power magnification image of vGLUT2 mRNA and c-Fos demonstrate the area of study (E). The boxed area in (E) is higher magnified in (F). High-power micrograph of c-Fos protein and vGLUT2 mRNA demonstrates a co-expression in the MePD (G). Many c-Fos-ir cell contain vGLUT2 mRNA. Location of (G) is illustrated by the quadrangle in (F). Scale bar 2 mm in (A); 1 mm in (B and E); 200 µm in (F) and 50 µm in (G).

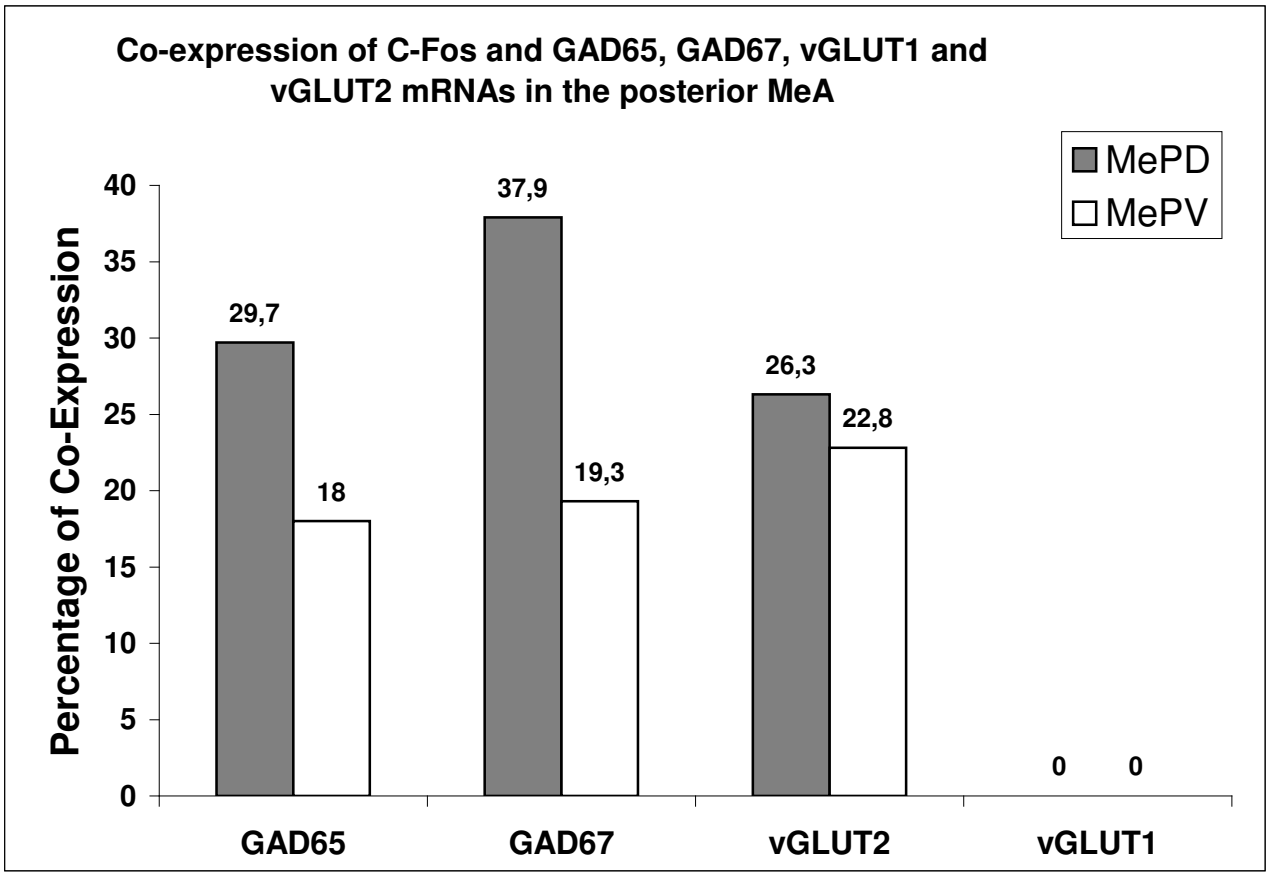


**Fig. 25 Percentage of Fos protein co-expression with mRNAs encoding GAD65, GAD67, vGLUT1, and vGLUT2 in the posterodorsal and posteroventral parts of the medial amygdala of juvenile stimulated rats**

Histograms represent the percentage of c-Fos-ir cells in the MePD/MePV of juvenile stimulated rats, co-localising with either GADs or vGLUT1/2. GABAergic and glutamatergic neurons were detected by in situ hybridisation. About 30% of the c-Fos-ir neurons in the MePD and 18% in the MePV were GAD65 positive. 38% and 19%, respectively, of the c-Fos-ir neurons in the MePD and MePV were expressing GAD67. Also,

26% of the c-Fos-positive neurons in the MePD and 23% in the MePV were vGLUT2 positive. VGLUT1 expressing neurons were not detected in this area of the amygdala.

### 6.1 Co-localisation of c-Fos with GAD65 and 67

511 c-Fos-ir neurons were counted in the MePD (Fig. 21) and MePV (Fig. 22) of the JS group. 29.8% of all c-Fos-ir neurons quantified in the MePD (33 of 111) expressed GAD65 mRNA (Fig. 25). By contrast, in the MePV, only 18% of c-Fos positive cells co-expressed GAD65 (31 of 172). By comparison, neurons double-labelled for GAD67 and c-Fos (Fig. 23) were only slightly more abundant (Fig.25) than those co-expressing GAD65 mRNA, namely 38% (55 of 145) in the MePD and 19.3% (16 of 83) in the MePV.

### 6.2 Co-localisation of c-Fos with vGLUT1 and vGLUT2

To study c-Fos positive cells double-labelled for vGLUT2, 241 c-Fos-ir neurons were counted in the dorsal and ventral parts of the posterior medial amygdala (MePD, MePV). Among these neurons, 24% (59 of 241) co-expressed vGLUT2 (Fig. 24).The co-expression pattern of c-Fos with vGLUT2 in the ventral and dorsal parts of the posterior medial amygdala was similar. In the MePD, 26.3% (31 of 118) of the c-Fos-ir cells were labelled for vGLUT2 mRNA (Fig. 25). In the MePV, 23% (28 of 123) of the c-Fos-ir cells were vGLUT2 positive. VGLUT1 expression, however, was detected in neither the MePD nor the MePV. In contrast to the Me, numerous neurons expressing vGLUT1 mRNA were observed in the PMCo and AHi. In these regions, most c-Fos-ir cells also expressed vGLUT1. Approximately 70% of the c-Fos-ir neurons in the posterior amygdala expressed vGLUT1 mRNA (data not shown).

## 7. Co-expression of c-Fos and oxcytocin or vasopressin in the activated regions in social recognition

To investigate whether the medial amygdaloid and the BNST areas activated during juvenile stimulation contain the neuropeptides vasopressin and oxcytocin, double labelling immunocytochemistry was performed. By immunocytochemistry, some vasopressinergic neurons were observed in the medial amygdala and BSTMP. Immunocytochemical double

labelling with arginie vasopressin and c-Fos did not show any co-expression in the medial amygdala and BSTMP. Furthermore, the medial amygdaloid nuclei, MePV and the BSTMA were devoid of oxcytocinergic neurons.